IMPLEMENTATION OF SIMPLE ADAPTIVE CONTROL AS A HYBRID CONTROL STRATEGY FOR A SEISMICALLY ACTIVE CABLE-STAYED BRIDGE

A Thesis

by

SNEHA AKKINENI

Submitted to the Office of Graduate and Professional Studies of
Texas A&M University
in partial fulfillment of the requirements for the degree of

MASTER OF SCIENCE

Chair of Committee, Luciana R. Barroso
Committee Members, John Niedzwecki
Luis San Andres
Head of Department, Robin Autenreith

August 2018

Major Subject: Civil Engineering

ABSTRACT

The motion of structural systems is a major challenge faced in the field of structural engineering. Certain measures such as the application of passive, active and semi-active control devices as a solution to overcome the motion of seismically critical structures has been the most preferred solution in recent times in the field of earthquake engineering. The advantages offered by control devices in terms of reliability, serviceability and reduced long-term costs has led to their popularity.

The current work presents the study of the performance of Quincy Bayview Bridge, a cable-stayed bridge located in Illinois. For a cable-stayed bridge, the deck-tower connections and abutments form the essential locations for assessment on the onset of a seismic activity. Therefore, the 3-span long continuous bridge consists of High Damping Rubber Bearing (HDRB) isolators and Magnetorheological Dampers (MR Dampers) located at the transverse and longitudinal directions to link the deck with towers and abutments. Simple Adaptive Control (SAC) is implemented into the MR Dampers as the control algorithm.

The primary objective is to evaluate the performance of an uncontrolled cable-stayed bridge system with a bridge system integrated with passive hybrid (Linear Viscous Dampers and HDRB) and semi-active hybrid control (MR Dampers and HDRB). The uncontrolled and controlled bridge is analyzed for two historic seismic excitations – the 1940 El Centro Earthquake and the 1994 Northridge Earthquake. The work also focuses on analyzing and comparing the results of the hybrid control system to the system controlled solely by passive and semi-active devices. An additional passive strategy (passive-on and passive-off) is implemented to evaluate and compare the performance of an MR Damper with hybrid control. Moreover, to lessen the

computational efforts, a reduced finite element model is created to capture the modal behavior of the complete structure and is investigated further to capture its dynamic performance.

The response reduction with the hybrid control strategies was found on par with the passive and semi-active devices that validates the efficiency of hybrid control. A similar response of the MR Damper controlled with SAC and passive-on is observed as the former delivers performance with its highest capacity. The difference in peak response percentage reduction between the full and reduced model validates that the reduced model cannot be substituted for the complete model due to its inefficiency to capture the geometric and material non-linearity in addition to its complete dynamic behavior.

DEDICATION

To Amma, Nanna and Amamma for being there for me, always.

ACKNOWLEDGEMENTS

First and foremost, I would like to thank my Advisor, Dr. Luciana R. Barroso for giving me an opportunity to be a part of her amazing research team and for her valuable advice and stellar guidance throughout the course of my research. Her energy and positive attitude has always motivated me to explore and learn something new constantly as part of our interactive research meetings and her courses.

None of this would have been possible without Rachel who was extremely helpful when I faced hindrances during the entire course of my research work.

I'm thankful to my family– Amma, Nanna, Raaga and Meghana for sending me this far from home to pursue my interests and for having faith in me that I would work to the best of my capabilities; My grandparents and friends for their unconditional love and support.

Last but not the least, I would like to extend my gratitude to Texas A&M University for being the most important part of my learning curve in life.

CONTRIBUTORS AND FUNDING SOURCES

This work was supervised by a thesis committee consisting of Professor Luciana R. Barroso and Professor John Niedzwecki of the Department of Civil Engineering and Professor Luis San Andres of Mechanical Engineering. All work for the thesis was completed independently by the student.

TABLE OF CONTENTS

Page

LIST OF FIGURES

Page

LIST OF TABLES

Page

1. INTRODUCTION

Environmental disturbances such as earthquakes and wind have been an essential area of study for their effect on structural infrastructure. These have enormous impacts on social and economic lives of the society. Most of the damages come from the disruption of urban habitation as well as damage to transportation and energy facilities and other utility services. For example, the 1994 Northridge Earthquake (moment magnitude 6.7) is known to have caused an overall loss of $40 billion with a structural damage of 38.8%. It killed 57 people and injured approximately 10,000 people (Tierney, 2002). The 1940 Imperial Valley earthquake (moment magnitude 6.9) caused a direct damage of $6 million, injuring 20 people and killing 9 people. It caused 60% of building damage and produced widespread disruption of irrigation systems (Earthquake Data Center, Southern California). The 1995 Kobe earthquake affected an area of four million people. It structurally destroyed 100,000 buildings and partially damaged 183,000 buildings. The 6.9 magnitude (moment magnitude) earthquake killed 6434 people and left 43,792 injured (Horwich, 2000). The Hanshin Expressway in Kobe experienced severe damage that resulted in the roll-over of an elevated section of the bridge.

The conventional design of structures such as buildings and bridges involves consideration of gravitational loads and lateral loads. While the design of structures for resisting gravitational loads can be a rather simplified process, developing a lateral force resisting system can be quite challenging. Structural strength and ductility to resist lateral forces can be attained by increasing the member sizes and the damping ratios. But, such an approach also leads to the rise of constructional cost. In order to overcome such additional expenses, research has been carried out to develop devices that can withstand these lateral forces and dynamic loading. The control

systems help in dissipating energy released as a result of wind and seismic excitation. The common practice nowadays has been the implementation of man-made control systems that are designed and chosen as per structure requirement.

1.1 Literature Survey

In the initial part, relevant work carried out in modeling the cable stayed bridges has been discussed. The latter part of the section deals with the control devices and algorithms that have had application for seismic control of structural systems.

1.1.1 Finite Element Modeling

The finite element modeling of a cable-stayed bridge can be quite challenging as there is no distinct procedure to capture the best behaviour of such superstructures analytically. Numerous modeling variations and assumptions have been executed to acquire the dynamic response of the cable-stayed bridges.

A comparative analysis of cable-stayed bridges for different layout conditions has been presented by Valdebenito et al (2012). Different structural configurations were developed based on variations of stay spacing, deck level and cable arrangement. Modal analysis was performed and compared to different layouts considering the modified matrix from the static nonlinear analysis. The work carried out by Valdebenito and Aparicio (2008) focused on the effect of variation of prestressing forces in the stay cables, using the response spectrum method. It was concluded that the low-to-moderate variations of the prestressing forces do not have a significant effect on the response of a seismically active cable-stayed bridge.

Asgari et al (2013) developed a three-dimensional finite element model of Tatara Bridge, a long span cable-stayed bridge located in Japan. Various assumptions such as a single-spine model for the deck, 3-D elastic elements for the towers, single-cable elements with appropriate boundary conditions for the deck-tower connections were implemented using ANSYS commercial programme. A sensitivity analysis was also performed to study the reliability of the finite element model. A similar finite element study has been carried out on the Owensboro cable-stayed bridge over the Ohio River by Kentucky Transportation Center (2006). The variations and complexity of the cable-stayed bridge led to the uncertainties of geometry and material. Assumptions were made for towers and girders to capture the best dynamic behavior of the bridge.

The finite element model of the Quincy Bayview Bridge for dynamic analysis was carried out by Wilson and Gravelle (1991) to investigate the dynamic response of the cable-stayed bridge. A simplified lumped mass model of the bridge was adopted to perform the non-linear static analysis. Additionally, the predicted model behaviour is compared with the results obtained from the ambient vibration measurements for the full-scale structure of the cable-stayed bridge.

Cable-stayed bridges are known for their long spans. Hence, such superstructures require time and effort to be analytically and computationally analyzed due to the presence of the increased number of control devices. However, no attempts have been made to reduce the model of the structure to ease computational effort. This research tries to lay focus on reducing the model of the bridge while simulating the behavior of the full-scale bridge structure.

1.1.2 Structural Control

The structural control systems can be broadly classified, based on the devices used, as passive, active and semi-active. The application of passive, semi-active and active control devices

as a solution to overcome the motion of seismically critical structures has been the most preferred solution in recent times in the field of earthquake engineering. The advantages offered by control devices in terms of reliability, serviceability and reduced long-term costs has led to their popularity.

1.1.2.1 Passive Systems

The passive systems refer to devices that are adapted for a known dynamic loading and capacity. They are tuned as per requirement and fail to perform efficiently for any other input and loading. Seismic isolators such as elastomeric bearings, lead-rubber bearings and dissipation devices like tuned mass dampers, fluid dampers fall under the category of passive control. However, these devices do not require external energy for operation and are known for their ease of design, mechanism and construction (Saeed et al., 2015).

Wesolowsky and Wilson (2003) studied the efficacy of seismic isolation in reducing the response of cable-stayed bridges. The isolated bridge produced 50% less base shear at the base of the towers compared to the non-isolated bridge. The optimal placement of passive systems for an improved performance of cable-stayed bridges has been studied by Hosam-Eddin and Abdel-Ghaffar (1995). Another study conducted by Soneji and Jangid (2007) on seismically isolated cable-stayed bridges focused on the effects of soil-structure interaction by performing seismic analysis in the time domain using the direct-integration method. The study carried out by Dyke and Yi (2000) on single degree of freedom (SDOF) and multi degree of freedom (MDOF) systems using passive and active devices showed that there was no improvement in performance of passive devices with an increase in stories of the structure. Therefore, passive devices deliver optimized performance for narrow design considerations.

1.1.2.2 Active Systems

Active control systems are devices that provide the required amount of forces to counteract any incoming dynamic loading. They are adaptable and can be used for various frequency ranges. Devices such as active base-isolators and active mass dampers constitute the active control system. Nonetheless, these devices have huge power requirement from external sources that cannot be reliable during a hazardous event. These systems demand sensors and controllers that makes it a complicated system and can either add or remove energy to the system, resulting in instability of the structure.

As an active control system, Hybrid Mass Dampers (HMD) have been installed on the top floor; to study the seismic and wind response; of a forty-three-story complex triangular building. (Shiba et al., 1997). The performance of HMD is compared with that of an unbonded brace damper and a rotational variable damper installed on a fifteen-story building. Passive and Active control systems using H2/LQG control algorithm were compared for a SDOF and a MDOF Structures. The Passive and Active devices performed similarly for a SDOF system. However, for an MDOF system, the active controller delivered an improved performance than the passive device.

Hydraulic actuators have been implemented in a three-story building and its performance has been compared with the semi-active MR Dampers using time-history analysis (Bitaraf et al., 2012). The actuators alleviate the structural response, but it causes instability to the system, unlike the MR Dampers. A similar comparison has been made for a benchmark cable-stayed bridge with multi-support excitations by Dai et al (2003). The semi-active devices delivered improved performances with less power input, enhancing the behaviour of the bridge.

1.1.2.3 Semi-Active Systems

To overcome the deficiencies of the passive and active systems, the passive systems have been evolved to what is presently called as the semi-active device. These devices such as variable friction and orifice dampers, controllable liquid dampers and semi-active impact dampers have the capability to adapt to the variability in the dynamic excitation and incorporate these variations as input to the system. Semi-active devices have limited control capacity but the advantages and reliability offered by such devices make them the most preferred solution of seismic mitigation.

The modeling and control of MR Dampers for reduction of seismic response was studied by Dyke et al. (1996). The MR Damper, implemented using clipped optimal control, was employed in a three-story building. The advantages offered by the MR Dampers alleviated the response of the structure in comparison to the linear active control system. Simple Adaptive Control and Genetic-based Fuzzy control have also been used as control strategies for evaluating the performance of MR Dampers for a 6-story building (Bitaraf et al., 2010). The performance of the dampers greatly depends on the structural systems and earthquakes. A study on the performance of a resetting semi-active stiffness damper has been carried out by Yang et al. (2000) on a three-story building model. Resetting Semi-Active Stiffness Dampers (RSASD) and Switching Semi-Active Stiffness Dampers (SSASD) were implemented using the Lyapunov theory. The performance of RSASD was found to be superior to SSASD in suppressing the response of the building.

1.1.2.4 Hybrid Systems

In order to overcome the deficiencies of each control system type and to further decrease the impact of the dynamic action on the structure, hybrid control strategies have been adopted in

recent times. In such strategies, the passive systems are used to mitigate the major portion of the response and the active/semi-active systems can be used to further reduce the displacements and accelerations. Hybrid systems have proven to increase the efficiency in controlling the response and are less expensive. The reliability and lower power consumption offered by these systems have made them the most promising devices for seismic response mitigation (Saeed et al., 2015)

Park et al (2003) applied the concept of the active hybrid control system to a phase II benchmark cable-stayed bridge. Hydraulic actuators were used as active devices, implemented using Linear Quadratic Gaussian (LQG) control, along with lead-rubber bearings as a passive control system. MR Dampers with clipped optimal algorithm were also provided as additional devices to further mitigate the seismic response of the bridge. It was found that due to the presence of passive control system, the hybrid control system exhibited no sign of instability.

The efficiency of the semi-active hybrid systems on cable-stayed bridges was studied and compared with the uncontrolled model of the bridge (Soneji and Jangid, 2006). The hybrid strategy comprised of semi-active (MR Dampers) and passive devices (HDRB) were implemented at the abutment and pier locations of the Quincy Bayview Bridge in Illinois. MR Dampers (semi-active) were implemented using Lyapunov theory and were modeled based on Bouc wen model, Bingham model and modified Bouc-Wen model. A similar study was carried out by Soneji and Jangid (2006) using passive hybrid systems. The hybrid system of the viscous fluid damper with elastomeric and sliding isolation systems resulted in reducing the earthquake response of an isolated cable-stayed bridge.

Semi-active devices such as variable orifice dampers and controllable fluid dampers have been employed by Jung et al (2004) using a clipped-optimal algorithm along with lead-rubber bearings as passive devices on a cable-stayed bridge. The passive semi-active hybrid system

resulted in reducing deck displacements when compared to the active control system and uncontrolled model of the bridge.

1.1.2.5 Control Strategies / Algorithms

The control strategies that drive these control devices form an important part of the performance of semi-active devices. The control algorithm helps to determine the command voltage to operate the MR Dampers. Strategies such as bang-bang control (Feng and Shinozuka, 1990), Lyapunov theory (Brogan, 1991), modulated friction control (Inaudi, 1997) and clipped-optimal control (Dyke and Spencer, 1996) have been studied and implemented in semi-active devices.

The disadvantage of these control algorithms is that they fail to capture and act accordingly to the parametric changes in the structure. For this reason, there is a need and requirement for a control system that has the ability to integrate the unforeseen changes in the structural system and still enhance the performance of the structure. Therefore, the concept of Adaptive Control was developed as a solution to overcome these deficiencies.

Various studies have involved the comparison and evaluation of Simple Adaptive Control (SAC) with other existing semi-active control strategies to mitigate the seismic response. It has been shown that it delivers improved and desired performance of the semi-active devices such as MR Dampers when compared to the uncontrolled model of the structure (Bitaraf et al., 2010). The control strategy involves a tracking system where a plant (original system to be evaluated) is made to track the model (idealized system). The control strategy helps to calculate the forces generated by the MR Dampers for alleviating the response of the cable-stayed bridge.

The adequacy of SAC has been examined by implementing it with semi-active devices such as MR Dampers and has been compared with passive-on and Modified Clipped Optimal Control (MCOC) strategies. These control strategies have been implemented on a twenty-story building and the non-linear behaviour of SAC was found to improve the structural response (Bitaraf and Hurlebaus, 2013).

However, the application of SAC in hybrid control systems has not been explored yet. For this reason, SAC has been implemented as a control strategy to drive the MR Dampers. Therefore, the research focuses on the extent of effect SAC has when it acts in combination with another control system.

1.2 Objective of Research

One of the objectives of the research is to identify important design considerations that can aid in computational modeling of a base-isolated cable-stayed bridge to implement a hybrid control system.

The main objective is to evaluate the performance of a base isolated cable-stayed bridge system for two historic far-field and near-field seismic excitations– the 1940 El Centro Earthquake and the 1994 Northridge Earthquake, respectively. The base-isolated cable-stayed bridge is integrated with HDRB Isolators (passive), Linear Viscous Dampers (LVD) and MR Dampers (semi-active) that are implemented using SAC. The efficiency of the hybrid control strategies will be compared with the uncontrolled model of the bridge.

Another objective of the proposed work is to focus on analyzing and comparing the results of the hybrid control system to the system controlled solely by passive and semi-active devices. It

aims to investigate the individual performance of Simple Adaptive Control when it acts in combination with other control devices.

1.3 Significance of Research

The significant number of cable-stayed bridges present in the United States makes it important to develop measures in mitigating seismic response of flexible long-span bridges. This thesis lays importance on alleviating the response of these susceptible structures by proposing efficient possible solutions for mitigating seismic responses based on the existing control strategies. The motive of the work has been to come out with adequate and economical systems from the already existing control devices and algorithms. Additionally, a simplified model with certain assumptions of the full-scale structure is attempted to reduce computational time and effort.

From the existing control algorithms, adaptive control has started gaining popularity due to its simple, reliable and economic applications. Therefore, the scope of performance of SAC as a hybrid control strategy is explored. The application of this strategy can be extended to tall buildings that have an equal consequence of seismic exposure. The implementation of these control measures can aid in overcoming the social, economic and structural damage to life and property that has always been a major cause of concern.

2. CASE STUDY STRUCTURE: CABLE-STAYED BRIDGE

2.1 Description of the Bridge

In order to implement the hybrid control strategy, a cable-stayed bridge has been considered for the analysis. The Quincy Bayview Bridge is located over the Mississippi River in Illinois. The main purpose of the bridge was to alleviate the traffic demands over the Quincy Memorial Bridge. It connects the cities of West Quincy, Missouri and Quincy, Illinois and spans over a length of 1780 ft. with a main span of 900 ft. and two side spans of 440 ft. each (Modjeski and Masters).

The bridge is known for its hybrid design comprising of two H-shaped concrete towers and double-pane fan type cables that support the composite bridge deck made of steel and concrete. A total of 56 cables support the deck system of that 28 support the main span and 14 support each side span. The bridge is symmetrical about the vertical central axis and rests on a base of deep pile foundations. Hence, the towers are considered fixed and soil-structure interaction is neglected.

2.2 Finite Element Modeling

The finite element modeling of a cable-stayed bridge can be quite a challenging task as there is no absolute modeling criteria. The assumptions considered for the analysis depends on the type of structure, the members and the soil conditions. Cable-stayed bridges are known to exhibit geometric non-linearity due to the sag in the cables. Hence, a non-linear static analysis would be sufficient to capture the modal behavior of the bridge analytically. However, to account for the stiffness, the deformed body at the end of the non-linear load case acts as an initial state to carry out further analysis.

Figure 2.1 The Quincy Bayview Bridge, Illinois.
[https://en.wikipedia.org/wiki/Bayview_Bridge#/media/File:Bayview_Bridge]

A lumped-mass finite element model of the bridge is developed as per specifications in Wilson and Gravelle (1991). A finite element software package, SAP 2000, is used to model the Quincy Bayview Bridge. The deck and the towers are modeled using linear elastic beam elements whereas the cables are modeled using linear elastic truss elements. Further details regarding the modeling of the individual components has been explained in the following sections.

To ease computational effort, attempts are made to reduce the full-scale model. It has been assumed that the behavior of the full-scale structure can be simulated and studied by considering only one-half of the bridge. This assumption has been made due to the symmetrical structure of the cable-stayed bridge. Therefore, a reduced model is simulated considering only half of the complete bridge. A similar finite element analysis is carried out for both the full-scale and reduced models. The design considerations for the reduced model is discussed in section 2.2.4.2.

2.2.1 Deck

The cross-section of the concrete deck consists of the deck, five stringers, two main edge girders, and two parapets that act as traffic barriers. The deck is made of a 46.5 ft. wide precast posttensioned slab of 9in. thickness. The five steel stringers are placed in the transverse direction with a spacing of 7.25 ft. Floor beams are placed in the transverse direction to the edge main girders that are equally spaced at 30 ft.

The deck is modeled as a spine, composed of 29 beam elements, with material and modal properties as mentioned in Table 2.1 and Table 2.2, respectively. The main span elements have a length of 60 ft. and the elements of side span have a length of 63 ft. The single central spine consists of offset links that are rigid in nature, to accommodate the cable anchor points and the masses of the deck. The length of the rigid link is 20 ft. and is aligned orthogonal to the deck spine, in the horizontal direction. The weight of the deck per unit length was found to be 7959 lb/ft (Wilson and Gravelle, 1991).

Table 2.1: Material Properties assigned to the deck (Wilson and Gravelle, 1991).

Property	Material	Value
Modulus of Elasticity	Steel	4.32×10^9 lb/ft^2
	Concrete	6.43×10^9 lb/ft^2
Unit Weight	Steel	490 lb/ft^3
	Concrete	150 lb/ft^3
Poisson's ratio	Steel	0.3
	Concrete	0.25

The mass of the deck is lumped and is assigned to the nodes as per weight of the deck per its unit length. It is placed below the centerline of the deck, using rigid links of 2.67 ft., to simulate the eccentricity between the mass of the deck and center of rigidity. The translational masses and

corrective mass moment of inertia of the deck assigned to the nodes are tabulated in Table 2.3. To accurately simulate the shear center characteristics and the actual mass moments of inertia of the deck, the corrective mass moment of inertia has been calculated for the three principal directions and are assigned to the respective nodes of the deck.

The deck is assumed to be flexible in the longitudinal direction whereas as it is assumed to be connected rigidly in the transverse direction to the abutments and piers. The details of the deck-tower connections are discussed in section 2.2.4.

Table 2.2: Properties assigned to finite element model of the deck (Wilson and Gravelle, 1991).

Modal Property	Value
Vertical (I_{yy})	39.5 ft^4
Transverse (I_{zz})	2289 ft^4
Torsion (J_{eq})	3.14 ft^4
Cross-Section Area (A)	8.9 ft^2

Table 2.3: Translational Mass and Correction to Rotational Inertia assigned to the finite element model of the deck (Wilson and Gravelle, 1991).

	Translational Mass	Correction to Rotational Inertia
Main Span	238770 lb.	$\Delta_x = -7.76\times10^7$ lb ft^2
		$\Delta_y = 1.66\times10^8$ lb ft^2
		$\Delta_z = 5.49\times10^7$ lb ft^2
Side Span	250778 lb.	$\Delta_x = -8.15\times10^7$ lb ft^2
		$\Delta_y = 1.89\times10^8$ lb ft^2
		$\Delta_z = 7.21\times10^7$ lb ft^2

2.2.2 Towers

The bridge consists of two concrete H-Shaped towers. Figure 2.2 illustrates the cross section and elevation of the tower. Each tower is at a height of 232 ft. above waterline. The concrete

tower is composed of two legs, an upper strut and a lower strut. The upper strut connects the upper portion of the towers whereas the lower strut supports the deck. The towers with dimensions 14.5 ft. x 7 ft. remains constant throughout but the cross section of the towers varies along the height and is divided into three sections. Section-1 refers to the lower portion of the deck consisting of the concrete legs and 4 ft. thick stiffening wall between the legs. Section-2 refers to the portion of the tower from lower strut to 15.5 ft. above the deck. In this section, the cross section of the tower has a centrally located hole of diameter 2 ft. Section-3 refers to the remaining segment of the tower above the lower strut. It consists of a rectangular hole of dimension 3 ft. x 8.5 ft.

The finite element modeling of the towers is done using rectangular frame elements with section properties specified in Table 2.4. To simplify the modeling of the tower, it is divided into 26 beam elements, including upper and lower strut. The mass of the tower is lumped and is assigned to the nodes based on the area and length of the column sections. The material properties of the tower are same as that of the deck. The stiffening wall acting as a web between the lower legs of the tower is considered as part of section-1 of the tower. Hence, the numerical values of section-1 are comparatively higher than rest of the sections.

Table 2.4: Sectional Properties of the tower (Wilson and Gravelle, 1991).

	Area (ft^2)	**I_{xx} (ft^4)**	**I_{yy} (ft^4)**	**J (ft^4)**
Section -1	192.5	15000	1900	1587
Section -2	94.4	410	1774	1145
Section -3	76.0	395	1625	892
Upper Strut	68.5	854	1550	1603
Lower Strut	78.0	954	1622	1736

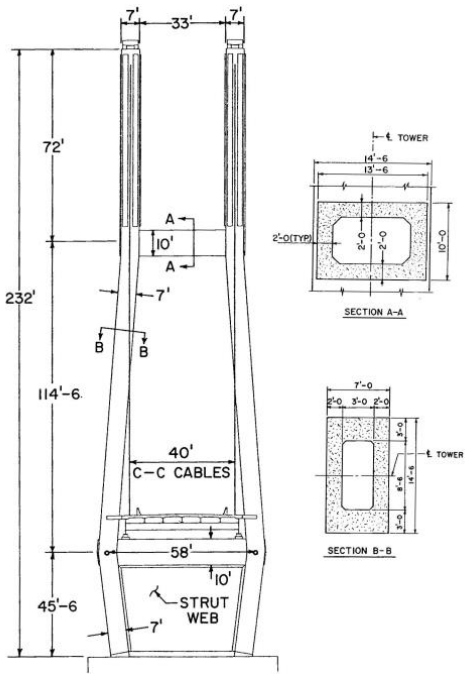

Figure 2.2: Elevation and cross-section of the tower (Wilson and Gravelle, 1991)

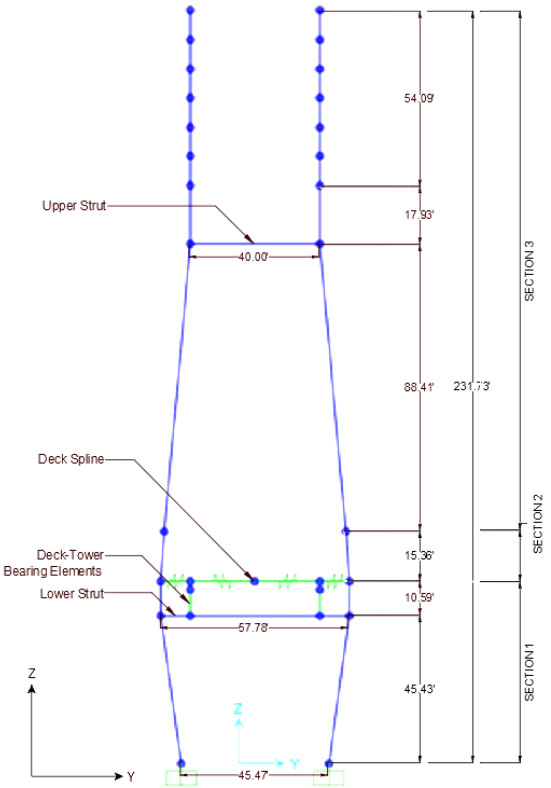

Figure 2.3: Finite element model of the tower.

2.2.3 Cables

The 56 cables supporting the deck are created using circular frame members that are modeled as truss elements. They belong to the fan type cable arrangement class of the cable-stayed bridges. To model the cables as trusses, M2 and M3 releases are assigned at both the ends and torsional release is assigned at one end of the frame element. In order to reduce the computational time, the cables are modeled as a single truss element. To maintain the flexibility of the deck, no restraints are assigned at the ends of the cables.

Cables are known to exhibit highly non-linear behavior due to geometric non-linearity. To account for the stiffness properties of the cables, Wilson and Gravelle (1991) designed the cables for a material of modulus of elasticity, based on an approach by Gimsing (1983) that is less than the actual modulus of elasticity of the cables. It was found that the behavior of the cables was captured for an equivalent modulus of elasticity of $E = 30 \times 10^6$ psi.

The cable system comprises four different configurations that vary based on the cross-section area and cable weight. The details of the properties used to design the cables are described in Table 2.5. They are spaced at 9 ft at the top of the towers and are equally spaced on the deck with 60 ft. on the main span and 63 ft. on each of the side spans. To model the axial load carrying behaviour of the cables, internal effects such as temperature loads are applied uniformly along its length. A thermal coefficient of $\alpha = 6.5 \times 10^{-6}$ /F is assumed to arrive at a temperature load of 984.615 °F and is applied to all the cables.

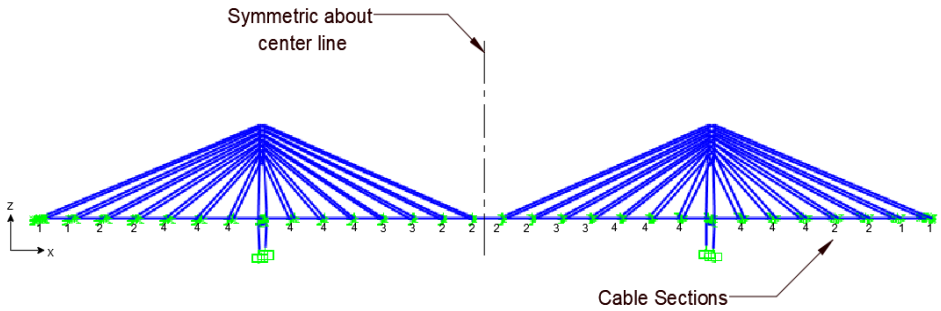

Figure 2.4: The cable arrangement for Finite Element Model.

Table 2.5: Cable Properties for Finite Element Model.

Cable number	Cable cross section area (ft^2)	Cable weight (lb/ft)	Weight per unit volume (lb/ft^2)
1	0.097	60.90	630.91
2	0.073	52.70	722.74
3	0.058	48.50	839.42
4	0.038	35.60	949.33

2.2.4 Connections at Deck-Tower and Abutments

The deck is assumed to be flexible along the longitudinal direction and rigid in the transverse direction due to the conventional bearings at the deck-tower connections. Both the towers are modeled identically. To capture the rigidity of the deck, the deck-tower connections are assigned bearing links. Each tower consists of 4 bearing links that are restrained in all the three translational directions and also along the x- and z- rotational direction, to connect the tower and the deck as shown in Figure 2.5. Two of them extend from the offset links of the deck to the leg of the tower. Another set of vertical bearing links connect the lumped masses of the deck to the lower strut. Therefore, the links provide relative motion between the deck and the tower about the transverse direction. Due to the pile foundation at the base of the tower, the ends of the towers are assumed to be fixed. Therefore, all the six degrees of freedom at the tower base are restrained.

2.2.4.1 Abutment Connection: Full-Model of the Bridge

It is a common practice to assign roller supports to the ends of long-span bridges, but in order to capture the accurate flexibility of the Quincy Bayview Bridge (Wilson and Liu, 1991), the ends have been modeled differently. To simulate the behavior of the ends of the deck, the nodes at the abutments are assumed to be restrained in all the three translational directions and also rotation about the transverse and vertical directions i.e., rotation only along the transverse (y-axis) and vertical (z-axis) directions is allowed. Both the ends of the deck are modeled similarly. A full-scale model of the cable-stayed bridge is shown in Figure 2.6.

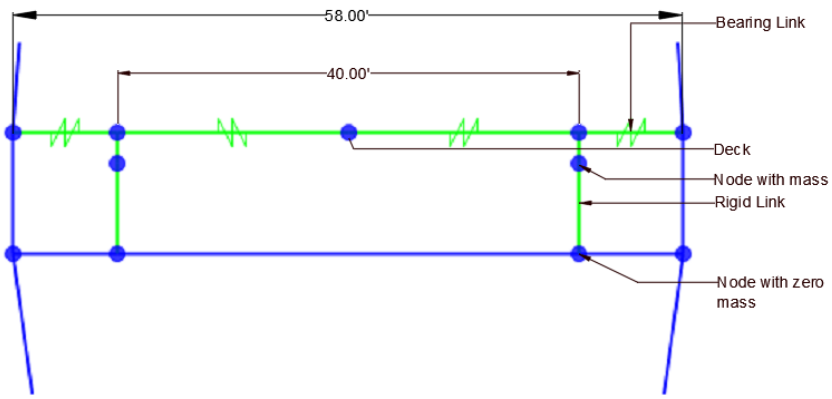

Figure 2.5: The deck-tower connection for the finite element model.

2.2.4.2 Reduced-Model of the Bridge

As stated before, to reduce computational effort, a reduced model of the Quincy Bayview Bridge is created by considering only half of the structure i.e. from one end of the bridge to its mid span (Figure 2.7). This requires simulating the ends of the bridge accurately to capture the modal behavior of the full-scale structure. To meet these requirements, joint springs of stiffness $33.85\ x\ 10^5$ lb/ft in the vertical direction and $4.77\ x\ 10^{10}$ lb/ft in the transverse direction are

assigned to the nodes at the end of the deck. The stiffness of the spring is calculated based on the load and deflection of the full-scale structure at the mid-span. The abutment of the bridge is modeled similar to the full-scale bridge.

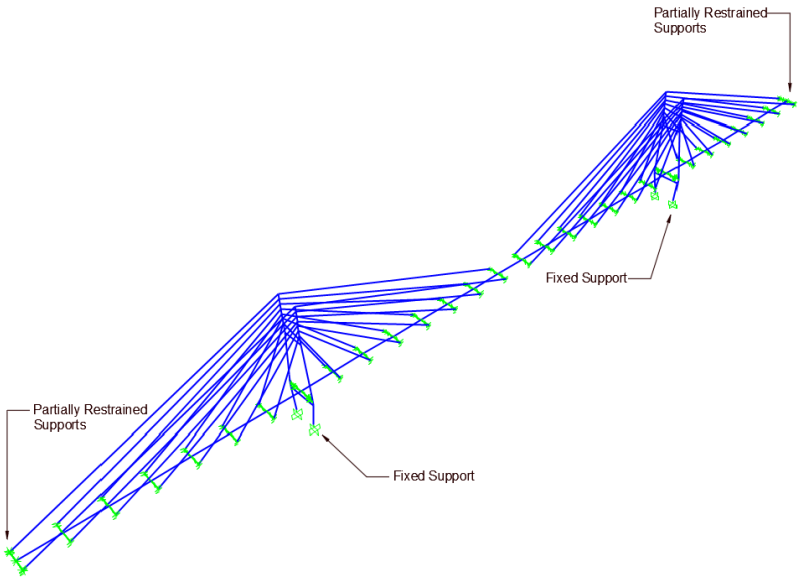

Figure 2.6: Full-scale model of the Quincy Bayview Bridge.

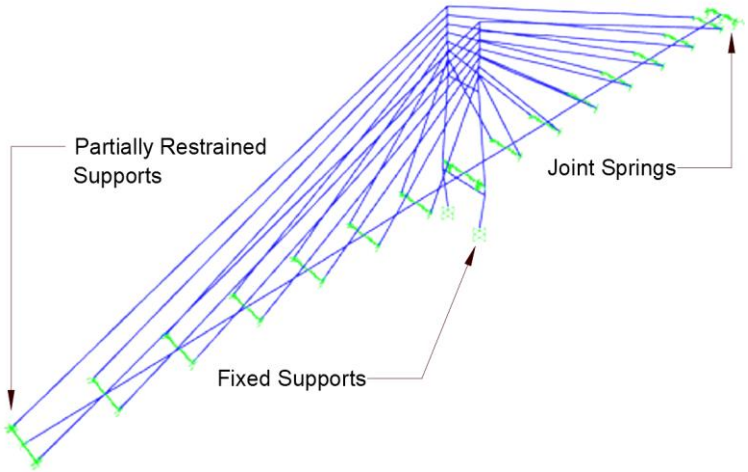

Figure 2.7: Reduced-model of the Quincy Bayview Bridge.

2.3 Modal Analysis

The modal analysis of the finite element model is carried out for the complete and reduced bridge structure to examine the modal properties and the behavior of the bridge. The static non-linear load cases for dead load and temperature load are created. To account for the stiffness of the model, modal analysis is carried out for stiffness at the end of the non-linear load case. P-delta effects are enabled to take into account the geometric non-linearity exhibited by the bridge structure.

2.3.1 Full-Model of the Bridge

To validate the approximation of the modal behavior of the full-scale model of the bridge, the properties obtained from the finite element software are compared with the ambient vibration measurement carried out by Wilson and Liu (1991) on the Quincy Bayview Bridge. A total of 10 modes are listed and compared for their time period, frequencies and mode shapes as obtained from SAP 2000, in Table 2.6. The mode characteristics captured for the first 10 modes of frequency range 0.37 Hz – 0.80 Hz substantiates the finite element model developed for the analysis. The fundamental period of 2.72 sec is obtained for the complete bridge structure and is associated with the vertical motions of the deck. The bridge also exhibits coupled torsion-transverse behavior in its third mode at a frequency of 0.50 Hz.

Table 2.6 also mentions the percentage error between the attained and experimental frequencies. The experimental values are obtained from the ambient vibration measurement study carried out by Wilson and Liu, 1991 on Quincy Bayview Bridge. The percentage errors can be pertained to the uncertainties in vibration tests and procedures for signal processing. The uncertainties arise from the dominant excitations due to wind, traffic and environmental factors

such as temperature and moisture. The experimental set-up to determine these frequencies consist of deployed hardware components such as data receiving system, cables and sensors that are prone to noise and errors. This affects the capability of the pre-processing and post-processing methods implemented for signal processing. But the ambient vibration measurements form the best source of validation for modal properties obtained from finite element analysis and are therefore used to compare the analytical values (Zhang et al.)

2.3.2 Reduced-Model of the Bridge

A similar analysis is carried out for the reduced-model of the bridge. The frequency, time period and modal shapes of the bridge is tabulated in Table 2.7. The mode shapes obtained for the reduced-model are found to be identical to the behavior exhibited by the full-model and the bridge model has a fundamental period of 2.05 sec. The vertical motion of the deck is captured by the first two modes of the bridge at frequencies 0.49 Hz and 0.50 Hz. The first torsional and transverse movement of the deck is attained at a frequency of 0.67 Hz.

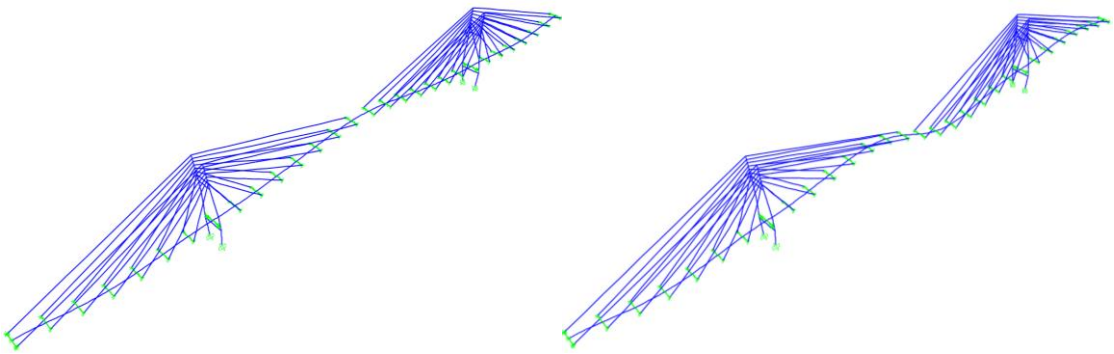

(a) Mode-1 (b) Mode-2

Figure 2.8: Mode-1 and Mode-2 of the full-model of Quincy Bayview Bridge

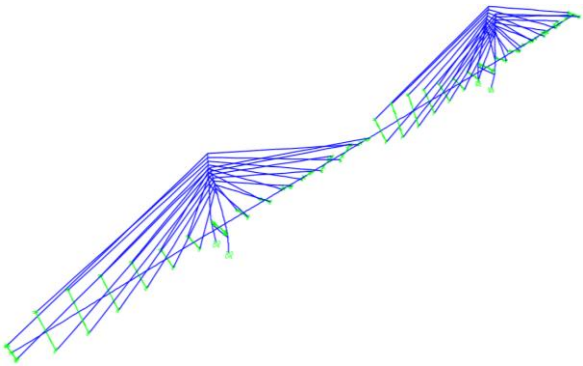

(c) Mode-3

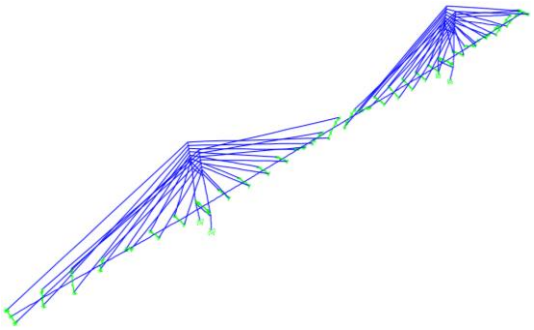

(d) Mode-4

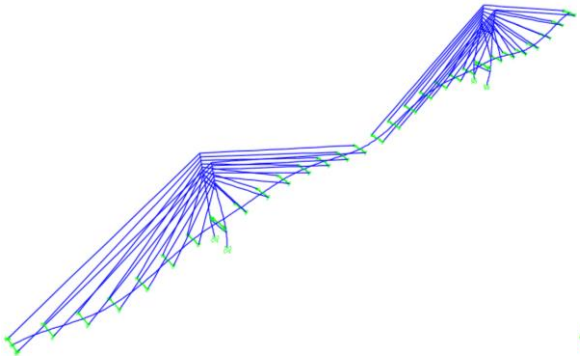

(e) Mode-5

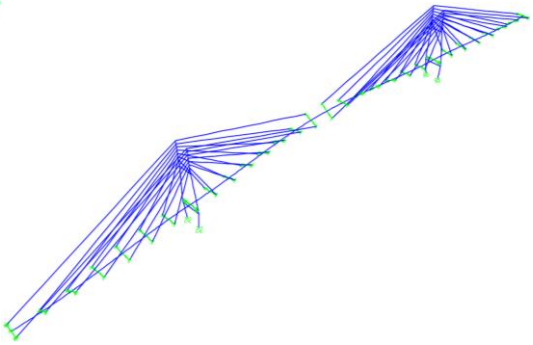

(f) Mode-6

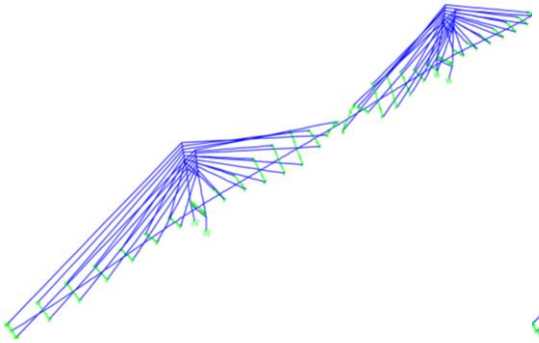

(g) Mode-7

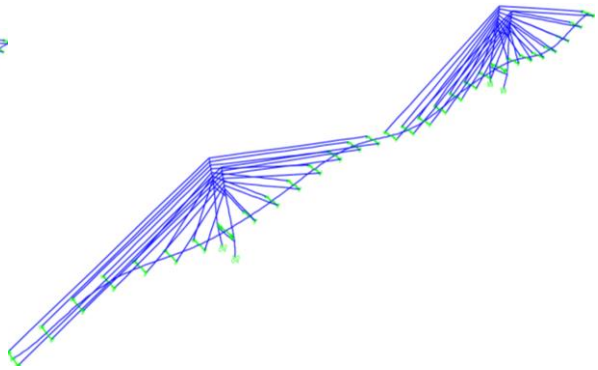

(h) Mode-8

Figure 2.9: Mode-3 to Mode-8 of the full-model of Quincy Bayview Bridge

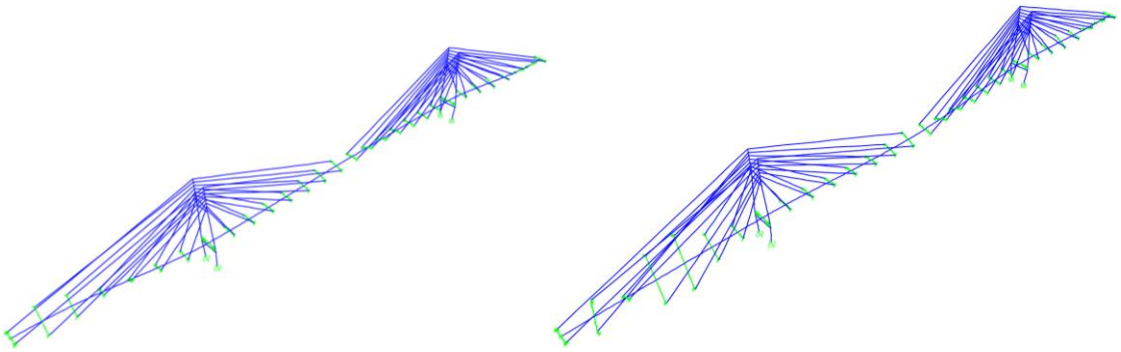

(i) Mode-9 (j) Mode-10

Figure 2.10: Mode-9 and Mode-10 of the full-model of Quincy Bayview Bridge

Table 2.6: Modal properties of full-model of the bridge.

Mode	Time Period FE Model (sec)	Frequency FE Model (Hz)	Mode Type	Experimental Modal Frequency (Hz)	Difference (%)
1	2.72	0.37	Vertical	0.38	1.95
2	2.03	0.49	Vertical	0.50	1.28
3	2.01	0.50	Torsion-Transverse	0.56	11.20
4	1.60	0.62	Torsion-Transverse	0.63	0.87
5	1.41	0.71	Vertical	0.70	-1.23
6	1.39	0.72	Torsion-Transverse	0.74	2.81
7	1.35	0.74	Torsion-Transverse	0.80	7.59
8	1.34	0.75	Vertical	0.80	6.49
9	1.33	0.75	Torsion-Transverse	0.89	15.58
10	1.26	0.80	Torsion-Transverse	0.89	10.46

Table 2.7: Modal properties of reduced-model of the bridge.

Mode	Time Period FE Model (sec)	Frequency FE Model (Hz)	Mode Type
1	2.05	0.49	Vertical
2	2.02	0.50	Vertical
3	1.50	0.67	Torsion-Transverse
4	1.35	0.74	Torsion-Transverse
5	1.33	0.75	Torsion-Transverse
6	1.24	0.80	Torsion-Transverse
7	1.17	0.86	Torsion-Transverse
8	1.08	0.92	Vertical
9	1.05	0.96	Torsion-Transverse
10	0.99	1.01	Torsion-Transverse

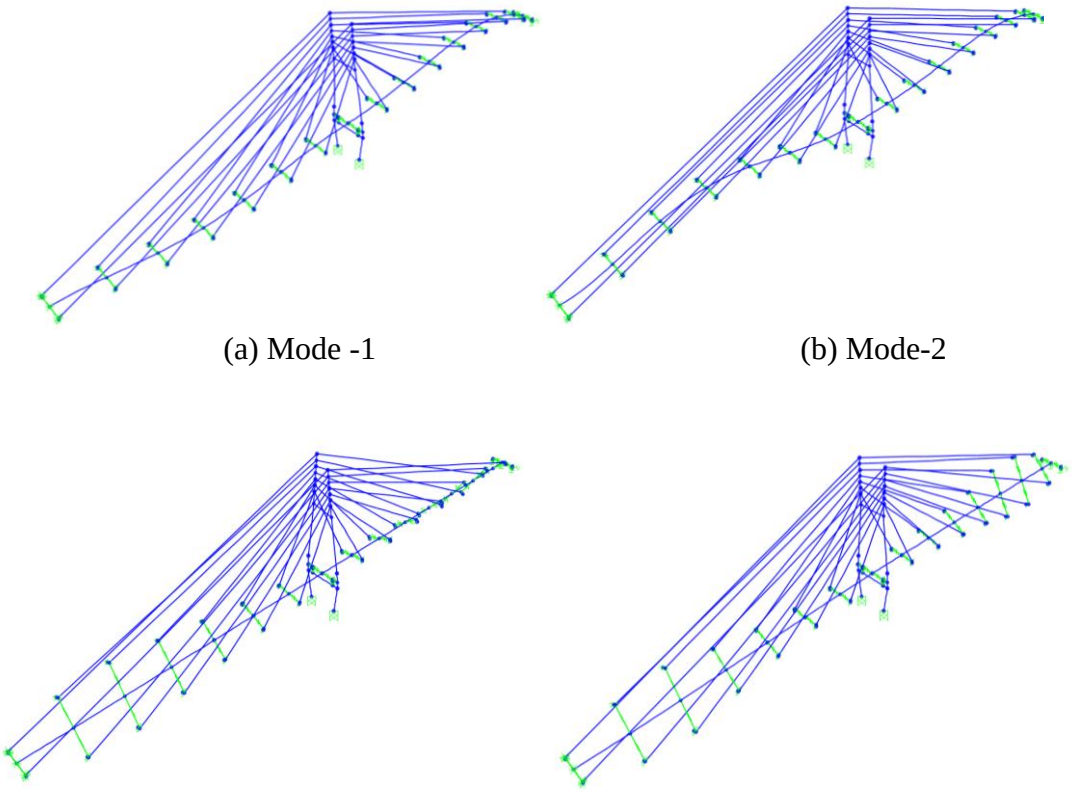

(a) Mode -1 (b) Mode-2

(c) Mode-3 (d) Mode-4

Figure 2.11: Mode-1 to Mode-4 of the reduced-model of Quincy Bayview Bridge

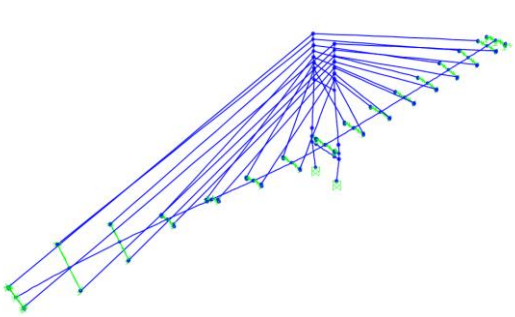

(e) Mode-5

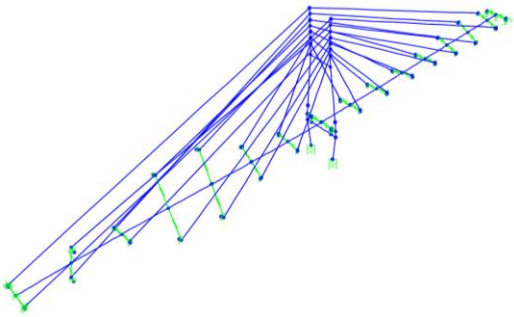

(f) Mode-6

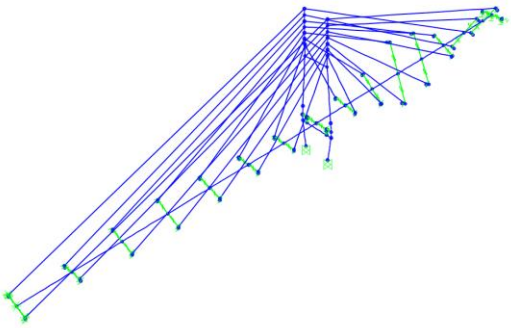

(g) Mode-7

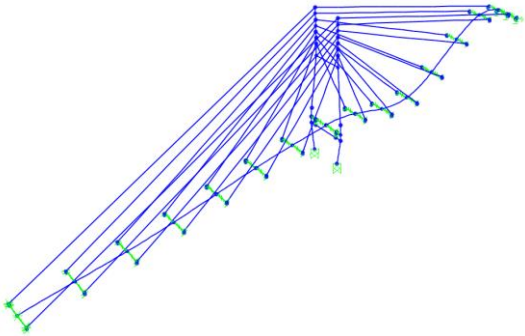

(h) Mode-8

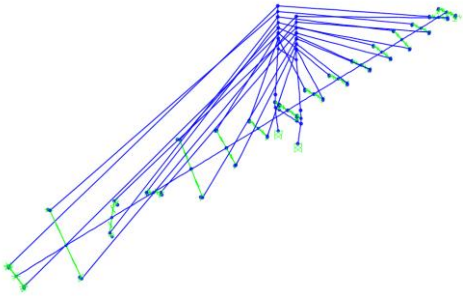

(i) Mode-9

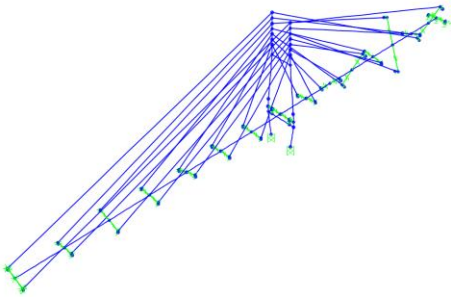

(j) Mode-10

Figure 2.12: Mode-5 to Mode-10 of the reduced-model of Quincy Bayview Bridge

The full-model is composed of 137 frame elements with 128 support members and 202 joints. The finite element model had a total of 420 degrees of freedom that were reduced to 294 using static condensation.

The reduced-model is the partial structure of the complete model of the bridge. In comparison to the full-model, the reduced-model produced a total of 216 degrees of freedom that were condensed to 153. It contained 69 frame elements with 68 support members and 106 joints.

3. SEISMIC EXCITATIONS

The two seismic excitations considered in this research are the 1940 El Centro Earthquake and the 1994 Northridge Earthquake. The El Centro occurred on May 18, 1940 in Imperial Valley, Southern California (Wikipedia, El Centro Earthquake). It struck with a moment magnitude of 6.9 along the Imperial Fault that is lined to the San Andreas Fault line, 5 miles north of Calexico in California. It affected the areas of Brawley, El Centro, Imperial, Mexicali and Calexico, California killing 9 people and injuring 20. The earthquake caused a damage of 60% of existing buildings such as public schools and office buildings and resulted in an overall damage worth $6 million (USGS). Figure 3.1 shows the acceleration-time record for the El Centro earthquake.

The 1994 Northridge Earthquake affected the populated region of Los Angeles, California. It occurred on January 17, 1994 with a moment magnitude of 6.7 along the Northridge blind thrust fault. It killed 57 people and injured more than 10,000. The epicenter of the earthquake was located at San Fernando Valley, 20 miles northwest of Los Angeles. The estimated damage was $40 billion, making it one of the costliest earthquakes that struck USA (USGS). Figure 3.2 shows the acceleration-time record for the Northridge earthquake.

Table 3.1 compares the characteristics such as Peak Ground Acceleration (PGA), duration, ground motion type and dominant frequency of the El Centro (Zahrai and Mortezaei, 2009) and the Northridge Earthquake (Celebi, 1995).

3.1 Response Spectra

The acceleration-time graph gives the measure of the ground motion caused by the earthquakes. The response of the structure to a seismic activity is highly dependent on its properties

such as damping ratio and time period. Thus, varying the time periods and damping ratios will give an overview of the behavior of the structure for a given earthquake. The peak displacements, velocities and accelerations of a structure form an important part in predicting its performance. Therefore, a theoretical approach of developing a design response spectrum is carried out to evaluate the dynamics of a structure that provides an input for the design in the building codes to overcome lateral forces such as earthquakes (Chopra, 2013).

The response spectra varies with damping ratio and is specific to an earthquake. Figure 3.3 shows the total acceleration (a measure of relative and ground acceleration) response spectra of the El Centro and the Northridge earthquake for a damping ratio of 1%. These response spectra provides an overview of possible structural systems that can get damaged in the event of an earthquake with a similar acceleration record.

In the present study, the 1940 El Centro and the 1994 Northridge earthquakes have been applied to the bridge system in both the orthogonal directions i.e. the x-direction and the y-direction as per the specifications in *AASHTO Guide Specifications in Seismic Isolation Design* (Guide Spec). Therefore, 100% earthquake excitation is applied along the y-direction and 30% is assumed to act along the x-direction (Anderson and Mahin, 2004).

Table 3.1: Characteristics of El Centro and Northridge

	El Centro Earthquake	**Northridge Earthquake**
Moment Magnitude	6.9	6.7
PGA (cm/sec^2)	313	578
Duration (sec)	31.18	59.98
Ground motion characteristic	Far-field	Near-field
Dominant Frequency (Hz)	0.39-6.39	2-3

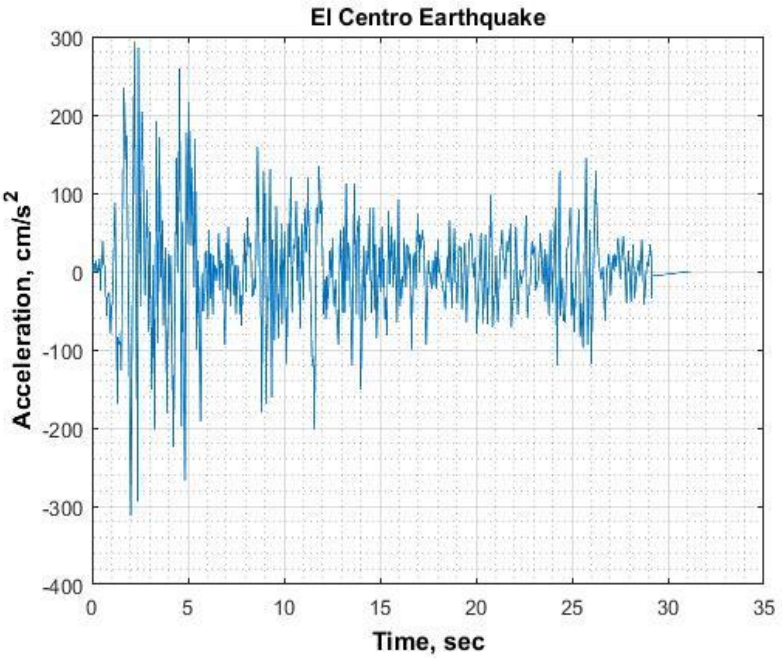

Figure 3.1: Acceleration record of the 1940 El Centro Earthquake

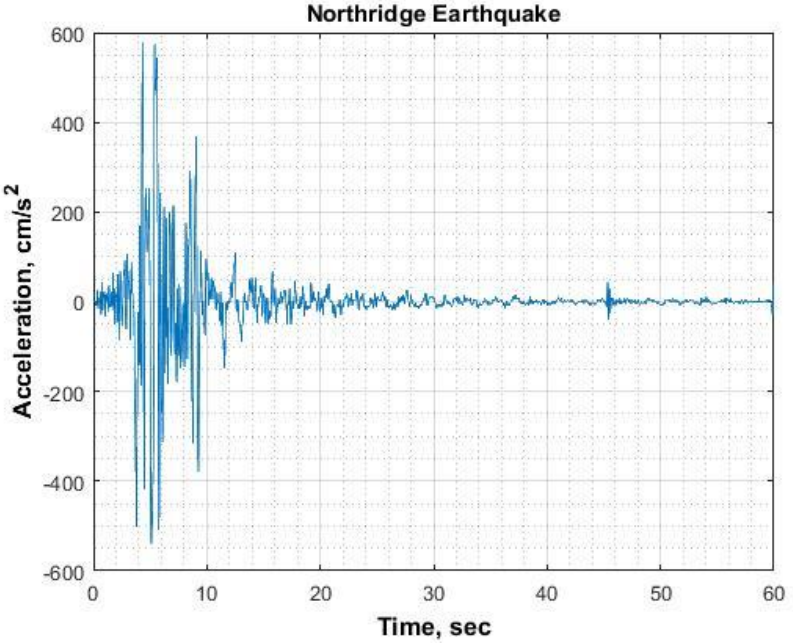

Figure 3.2: Acceleration record of the 1994 Northridge Earthquake

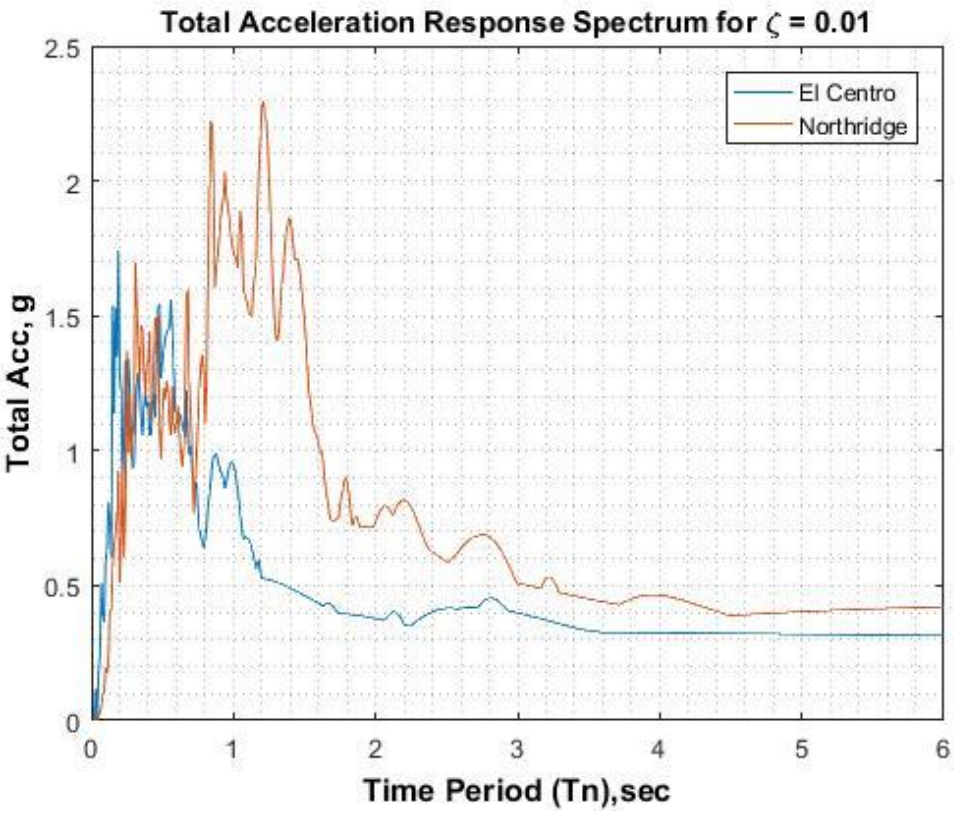

Figure 3.3: Acceleration Response Spectrum for $\zeta = 0.01$

4. CONTROL DEVICES

The advancement in technology has led to the development of devices that can be placed externally on a structural system to monitor the responses under the effects of lateral forces such as wind and earthquakes. The effectiveness of these devices has been a major research area in the field of structural motion control.

As discussed before, the control devices can be classified into three categories, namely, passive, active and semi-active. The control devices adopted as part of this research are the High Damping Rubber Bearings (HDRB) and Linear Viscous Dampers (LVD) that are used as passive devices and the Magnetorheological Dampers (MR Dampers) that are adopted as the semi-active control devices. Each set of devices has its own set of advantages and disadvantages. Therefore, to account for an improved performance, hybrid devices are adopted and compared for their efficiency with the passive and semi-active devices. The modeling, working and implementation of these systems in complex structures such as a bridge, is discussed in the following sections.

4.1 Passive Devices

Passive control systems refer to the set of devices that dissipate energy as part of their mechanism, hence they cannot cause instability. The capacity of these devices is controlled and tuned to deliver a performance for a limited input. They fail to adapt to the changes in the surroundings such as occurrence of earthquakes with a varied acceleration response or a different dynamic loading and alteration of structural parameters. However, these devices do not require external power source and hence this makes these more affordable with an ease to construct and

implement. In this study, HDRB Isolators and Linear Viscous Dampers have been implemented and studied for their performance and efficiency.

4.1.1 HDRB Isolators

HDRB isolators fall under the category of seismic isolation devices that offer flexibility in the longitudinal and transverse direction and are stiff in the vertical direction. The flexibility offered thus varies the fundamental modes of the structural system and shifts the system away from the periods of excitation (Saaed et al., 2013). HDRB is composed of alternate layers of vulcanized reinforcement of steel plates and rubber. These isolators are implemented commonly for structures with small to medium height and they exert force in both the horizontal directions, i.e. in the x-direction and y-direction. For the Quincy Bayview Bridge, the HDRB isolators are used to isolate the deck from the towers and are placed at the four supports of the deck. A total of 8 isolators have been implemented with 2 isolators at each support. The restoring forces developed by the HDRB can be represented as (Soneji and Jangid, 2006)

$$\begin{Bmatrix} F_x \\ F_y \end{Bmatrix} = \begin{bmatrix} c_b & 0 \\ 0 & c_b \end{bmatrix} \begin{Bmatrix} \dot{x}_b \\ \dot{y}_b \end{Bmatrix} + \begin{bmatrix} k_b & 0 \\ 0 & k_b \end{bmatrix} \begin{Bmatrix} x_b \\ y_b \end{Bmatrix} \tag{4.1}$$

Where x_b, y_b, $\dot{x}_b$ and $\dot{y}_b$ represent the displacements and velocities of the isolator in the x- and y-direction respectively. c_b and k_b denote the damping and stiffness of the isolators which are a function of damping ratio and isolator time-period. The time-period of the isolator is dependent on its stiffness and is calculated using

$$T_b = 2\pi \sqrt{\frac{m_d}{\sum k_b}} \tag{4.2}$$

And the damping ratio of the isolator is determined using mass of the deck m_d and isolation frequency ω_d that is equal to $2\pi/T_b$. The damping ratio is expressed as

$$\xi_b = \frac{\sum c_b}{2m_d\omega_b} \tag{4.1}$$

In this study, an HDRB with damping ratio of 10% and with an isolator time period of 2 sec, as implemented by Soneji and Jangid (2006), is adopted for the analysis.

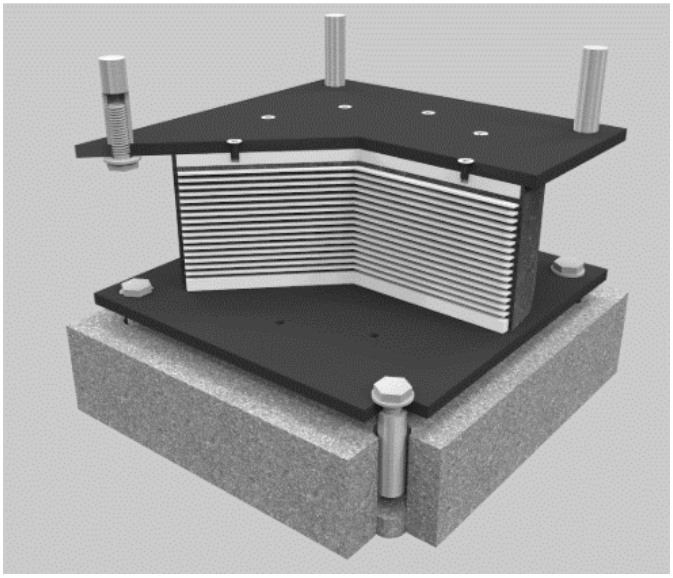

Figure 4.1: An HDRB Isolator (Doshin Rubber)

4.1.2 Linear Viscous Dampers

Linear viscous dampers are composed of plunger and external plates filled with viscous fluid. A typical viscous damper consists of a piston rod, an accumulator, control valve, piston head with orifices and a seal retainer as shown in Figure 4.2. When the position of the piston rod changes, a resisting force, that is dependent on the velocity of the rod, is exerted by the fluid

when it is forced through the orifice in the piston head. The damping force (F) exerted by such dampers is a function of its velocity ($\dot{u}$) and can be expressed as (Connor, 2003)

$$F = f(\dot{u}) \tag{4.2}$$

$$F = c\dot{u} \tag{4.3}$$

It can be linearly expressed as a product of the damping coefficient, c , of the viscous damper and its velocity. For a linear viscous damper, the damping coefficient remains constant. In the current study, an idealized linear viscous damper has been assumed with a damping ratio of 10% and are simulated to be placed at the deck-tower connections and at the abutments.

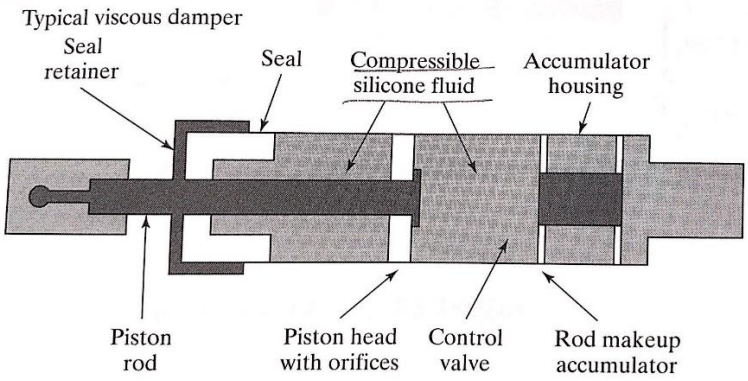

Figure 4.2: Components of a Viscous Damper (Connor, 2003)

4.2 Semi-Active Devices

Semi-active devices are a class of passive devices that have the capability to adopt to unpredictable disturbances in the structure. These devices are run by control algorithms that are adaptive in nature and are dependent on the input for the structure. These require small amount of external power source to keep the system stable. A semi-active system consists of various components such as sensors to estimate input and output, a control system to evaluate the response

and to develop control input to the actuators, a passive device and an actuator to regulate the passive device. Variable orifice and friction dampers, controllable tuned mass dampers and fluid dampers such as MR Dampers and Electrorheological Dampers (ER Dampers) are few examples of semi-active devices (Saaed et al., 2013).

4.2.1 MR Dampers

Magnetorheological Dampers fall under the category of controllable fluid semi-active devices. They are filled with MR fluid - composed of tiny iron particles that get polarized and align themselves when subjected to a magnetic field. MR Fluids are known to exhibit hysteretic behavior over a wide temperature range (-40 ^{o}C to 150 ^{o}C). Moreover, these dampers are preferred for their low viscosity and high yield strength (Dyke et al., 1996).

The MR Damper consists of an accumulator, MR fluid, a piston and a magnetic circuit as shown in Figure 4.3 and is controlled with an input voltage. The electromagnet that is placed in the piston head creates the magnetic field. To accurately capture the behavior of a MR Damper, various models have been developed to study the non-linearity exhibited by these devices as discussed in the following sections.

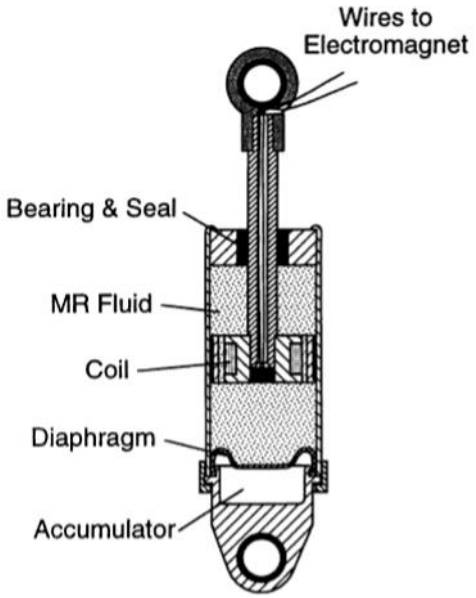

Figure 4.3: Components of a MR Damper (Dyke et al., 1996).

4.2.1.1 Bingham Model

Bingham model was initially developed to study the behavior of ER fluids (Shames and Cozzarelli, 1992) and was later implemented to analyze the non-linearity of MR Dampers. A viscous damper is placed in parallel with a coulomb friction element as depicted in Figure 4.4 and the force exerted by the damper (F) formed using Bingham model is given by

$$F = f_c \operatorname{sgn}(\dot{x}) + c_o \dot{x} + f_o \tag{4.4}$$

where f_c represents the frictional force that is dependent on the yield stress of the fluid, c_o represents the damping coefficient of the device and $\dot{x}$ represents the velocities of the piston. f_o is the offset provided in the force due to the presence of an accumulator. This model was implemented by Spencer et al., (1997) to study the force-displacement and force-velocity responses exhibited by the MR Damper. As a result of the study, this model was found to show

the absence of non-linear behavior in the force-velocity response and therefore was found to be inaccurate to capture the behavior of the damper for control analysis.

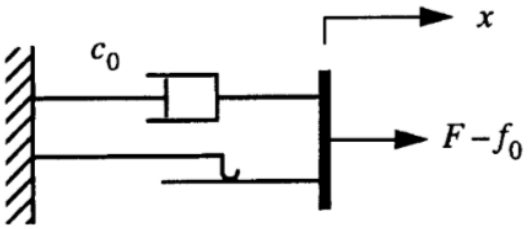

Figure 4.4: Bingham model proposed for an ER Damper (Spencer et al., 1997)

4.2.1.2 Bouc-Wen Model

To mathematically match the experimental behavior of the damper, simple Bouc-Wen Model was developed by Wen (1976) and is shown schematically in Figure 4.3. The Bouc-Wen model captures the hysteric behavior of the device that exerts a force given by the equation

$$F = c_o\dot{x} + k_o(x - x_o) + \alpha z \tag{4.5}$$

where x_o and k_o represent the initial displacement and stiffness of the spring and z is known as the evolutionary variable defined by

$$\dot{z} = -\gamma |\dot{x}| z |z|^{n-1} - \beta\dot{x} |z|^n + A\dot{x} \tag{4.6}$$

The model parameters γ, β, A are constants that define the prototype of a MR Damper. However, similar to the Bingham model, the simple Bouc-Wen model also fails to exhibit the non-linear behavior of the device for the force-velocity response. (Spencer et al., 1997).

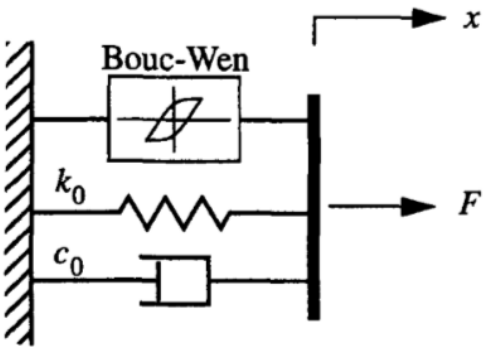

Figure 4.5: Bouc-Wen model for a MR Damper (Spencer et al., 1997).

4.2.1.3 Modified Bouc-Wen Model

To overcome the deficiencies of the Bingham model and the Bouc-Wen model and to mathematically capture the non-linear behavior exhibited by a MR Damper, a modified version of the Bouc-Wen model was developed as illustrated in Figure 4.6.

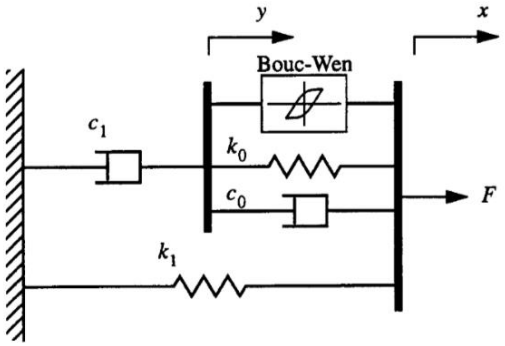

Figure 4.6: Modified Bouc-Wen model for a MR Damper (Spencer et al., 1997).

The total force produced by the device is given by summing the forces generated by the upper and lower half of the illustration. Considering the forces produced in the upper half of the system, we obtain

$$c_1\dot{y} = \alpha z + k_o(x - y) + c_o(\dot{x} - \dot{y}) \tag{4.7}$$

Rearranging, we get

$$\dot{y} = \frac{1}{(c_o + c_1)}[\alpha z + c_o\dot{x} + k_o(x - y)] \tag{4.8}$$

The evolutionary variable z is controlled by

$$\dot{z} = -\gamma\,|\dot{x} - \dot{y}\,|\,z\,|\,z\,|^{n-1} - \beta(\dot{x} - \dot{y})\,|\,z\,|^{n} + A(\dot{x} - \dot{y}) \tag{4.9}$$

The total force generated by the device is expressed as

$$F = \alpha z + c_o(\dot{x} - \dot{y}) + k_o(x - y) + k_1(x - x_o) \tag{4.10}$$

It can also be denoted as

$$F = c\ \dot{y} + k_1(x - x_o) \tag{4.11}$$

where k_1 is the accumulator stiffness and c_1 is the viscous damping in the model, x_o is the initial displacement of spring k_1 associated with damper force from the accumulator (B.B and R.S 2006). Spencer et al., (1997) proposed the dependence of viscous damping coefficients on the applied voltage (u) . The linear relation between them is given by

$$\alpha = \alpha_a + \alpha_b u \tag{4.12}$$

$$c_1 = c_1 a + c_1 b u \tag{4.13}$$

$$c_o = c_{o1} + c_{ob} u \tag{4.14}$$

The MR Dampers, in this study, are placed in the longitudinal and transverse directions at the four supports of the deck. The device is modeled as per the parameters specified in Soneji and Jangid (2006) using Modified Bouc-Wen Model to capture the nonlinearity exhibited by the device. To input the varying voltage into the device, the inverse of Simple Bouc-Wen Model is adopted. The voltage is applied as per the equation

$$u = \frac{f + c_{oa}\dot{x} - \alpha_a z}{c_{ob}\dot{x} + \alpha_b z} \tag{4.15}$$

where f corresponds to the input of the states from the structure. The modal parameters chosen for the analysis have been tabulated in Table 4.1. The MR Damper implemented has a total capacity of 1000 kN and is applied a voltage of 0 V - 10 V. The forces produced are saturated to meet the capacity of the damper.

For efficient mitigation of the seismic forces on a large-scale structure such as the Quincy Bayview Bridge, a total of 32 MR Dampers are installed for the full-model of the bridge and a total of 16 MR Dampers are adopted for the reduced-model of the bridge.

Table 4.1: Parameters for developing the model of MR Damper (Jangid and Soneji, 2006)

Parameter	Value	Parameter	Value
α_a	3.166 Kip/ft	γ	15.244 /ft^2
α_b	2.823 Kip/ft	β	15.244 /ft^2
c_{oa}	7.539 Kip/ft	η	100 /sec
c_{ob}	7.834 Kip-sec/ ft-V	x_o	0.5901 ft
c_{1a}	572.933 Kip-sec /ft	k_1	0.0006707 Kip/ft
c_{1b}	512.87 Kip-sec/ ft-V	A	1107.2
k_o	0.000134 Kip/ft	n	2

4.3 Hybrid Control Devices

To account for the disadvantages associated with the individual performances of passive, active and semi-active devices as mentioned previously, the concept of hybrid control systems has been gaining demand since the early 1990's (Saaed et al., 2013). In this research, a hybrid control system comprising of base isolation is implemented with semi-active devices such as MR Dampers placed on the superstructure. The concept of hybrid control system involves the base isolators to

dissipate maximum response of the system and the additional devices i.e. the MR Dampers to alleviate displacement and accelerations of the sensitive equipment on the superstructure.

The base isolators and the MR Dampers are chosen to be placed at deck-tower connections and at abutments due to the ease of installation and to mitigate the response at the critical joints such as the supports and connection between the components of the bridge.

5. CONTROL ALGORITHM

To drive the control devices for delivering a good performance, an efficient mechanism needs to be provided. In this research, the performance of the MR Damper is tested by implementing Simple Adaptive Control (SAC) as the control algorithm to drive the damper for structural response efficiency.

5.1 Simple Adaptive Control

Simple Adaptive Control is a developed version of Model Reference Adaptive Control (MRAC) concept. MRAC requires the model to be of the same order as that of the plant and are assumed to have full-state feedback. But unlike MRAC, SAC does not demand the model to be of the same order as the plant (Barkana, 2015). The desired state vectors that are to be controlled can act as an input to the system. It is evident from the name that SAC is adaptive in nature, which suggests that it can adapt to the changes in the external surroundings such as the variations in dynamic loading, alteration of the structural parameters such as reduced mass and stiffness of the system that occur as a result of corrosion or damage due to the previously occurred earthquakes.

The SAC algorithm revolves around the concept of a plant and a model. The plant refers to the structural system whose performance is to be controlled and the model refers to an idealized system that exhibits the desired performance. The idea involves the plant to be able to follow the model and deliver a satisfactory performance. For doing so, the algorithm requires to generate the output of plant and model and feed the error between the plant and model into the system to calculate the parameters necessary to bring the changes in the plant. The governing equations of model and plant for the control strategy are as follows (Bitaraf, 2011)

$$\dot{x}_m(t) = A_m x_m(t) + B_m u_m(t) \tag{5.1}$$

$$\dot{x}_p(t) = A_p x_p(t) + B_p u_p(t) + d_i(t) \tag{5.2}$$

where A_m and A_p are the state matrices of model and plant, B_m and B_p are the input matrices, C_m and C_p are the output matrices of the model and plant respectively. x_m and x_p correspond to the model and plant state vector. The output vector of model (y_m) and plant (y_p) can be expressed as

$$y_m(t) = C_m x_m(t) \tag{5.3}$$

$$y_p(t) = C_p x_p(t) + d_o(t) \tag{5.4}$$

where u_m is the input command vector and u_p is the input control vector. The input and output disturbances are represented by $d_i(t)$ and $d_o(t)$. The input control vector is the product of the adaptive gain $K(t)$ and the reference vector $r(t)$.

$$u_p = K(t)\begin{bmatrix} y_m - y_p & x_m(t) & u_m(t) \end{bmatrix}^T \tag{5.5}$$

that can be written as

$$u_p = K(t)\left[r(t)\right]^T \tag{5.6}$$

The adaptive gain is composed of the integral gain $K_I(t)$ and the proportional gain $K_p(t)$

$$K(t) = \begin{bmatrix} K_e(t) & K_x(t) & K_u(t) \end{bmatrix} \tag{5.7}$$

$$K(t) = K_I(t) + K_P(t) \tag{5.8}$$

The proportional gain is required to increase the plant performance, i.e to increase the rate of convergence of plant performance while the integral gain is necessary for tracking and stabilizing the system. They are expressed as

$$\dot{K}_I(t) = \left(y_m(t) - y_p(t)\right) r(t)^T T - \sigma K_I(t) \tag{5.9}$$

$$K_p(t) = \left(y_m(t) - y_p(t)\right) r(t)^T \bar{T} \tag{5.10}$$

The matrices T and $\bar{T}$ are the positive definite scale matrices that influence the rate of adaptation. The constant σ is included to limit the values of the integral gain. The block diagram illustrating the working of SAC is shown in Figure 5.1.

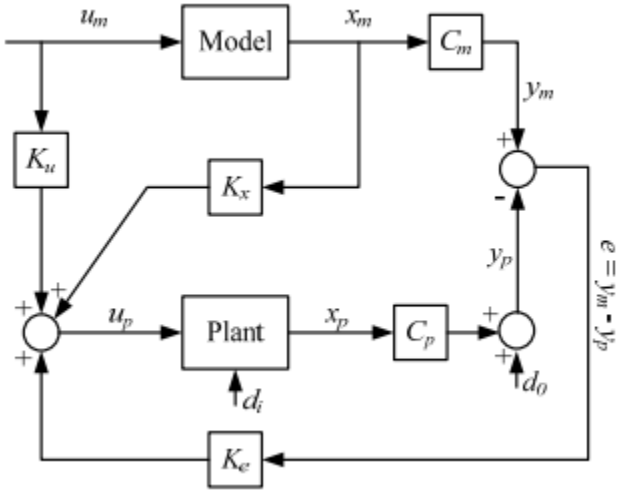

Figure 5.1: The schematic diagram of Simple Adaptive Control Mechanism (Bitaraf, 2011)

Here, the model is assumed to have the properties as that of the plant but the output of the model is instructed to decrease by 90%. Therefore, the mass, stiffness and damping matrices remain the same for the plant and the model. The seismic excitations serve as an input for both plant and model. The velocities and displacements of the model can serve as the input for the plant for its corresponding response reduction but, however, in this study, the model is commanded to decrease only the plant displacements for locations where the isolators are placed. Therefore, the

advantages offered by the simple adaptive control are put to use by obtaining responses only for the desired quantities.

In this study, the matrices for T and $\bar{T}$ are both assumed to be $10^8 I$ and $\sigma = 0.1$. The plant and model output are required to be of the same order since their difference acts as an input for the control algorithm. The output from SAC serves as the input for the MR Damper that controls the forces generated by the device. The performance of SAC and the damper also depends on the limitations exerted on its forces. The resultant forces from the MR Damper are saturated based on the capacity of the damper. Hence, the performance and the error between the plant and the model is a result of various factors. Therefore, the parameters for the optimum performance of SAC are to be chosen accordingly.

6. COMPUTATIONAL ANALYSIS

Superstructures such as cable-stayed bridges that involve complex structure and behavior are to be simulated into simple models using mathematical formulations and computational tools. This is achieved by arranging the model parameters into suitable form to carry out dynamic analysis. Therefore, tools such as MATLAB® and SIMULINK® are used to implement the large mathematical formulations involved in the design.

6.1 Equation of Motion

Using Newton's second law of motion, the resultant forces exerted on a structural system can be represented by its equation of motion. For any single degree of freedom system with mass, m, stiffness, k and a damping, c the equation of motion for the system can be expressed as

$$m\ddot{u} + c\dot{u} + ku = p(t) \tag{6.1}$$

where $p(t)$ denotes the external dynamic loading applied on the structure (Chopra, 2013). For a multi degree of freedom system of order N, the above equation turns into a system of N ordinary differential equations. The parameters in the equation are now vectors or a matrix of order N, where N is the number of degrees of freedom of that particular system. For an MDOF system, the mass, stiffness and damping matrix are developed for the active DOF's of the system.

For an earthquake excitation with a ground acceleration, $\ddot{u}_g$, the equation of motion can be denoted as

$$m\ddot{u} + c\dot{u} + ku = -m\ddot{u}_g \tag{6.2}$$

where $\ddot{u}_g = \{\ddot{u}_x \quad \ddot{u}_y \quad \ddot{u}_\theta\}^T$ represents the x, y and rotational components of the ground acceleration.

For the Quincy Bayview Bridge, the mass matrix of the bridge is represented by a diagonal matrix with the masses of the nodes present in the model arranged along its diagonal. The off-diagonal terms in the stiffness and damping matrices are composed of coupled damping terms from the respective contributing DOF's. Finite element software packages such as SAP2000 generates the mass and stiffness matrices of the system for the active, restrained and constrained degrees of freedom. In order to carry out dynamic analysis, DOF's with zero mass are to be removed. Therefore, static condensation is applied to remove the rotational DOF's that have a zero mass along the diagonal as an earthquake excitation does not exert forces along these DOF's. But these DOF's contribute towards the stiffness of the system. Hence, the resultant condensed stiffness matrix is developed using the following formula (Chopra, 2013)

$$\hat{k}_{tt} = k_{tt} - k_{0t}{}^T k_{00}{}^{-1} k_{0t} \tag{6.3}$$

where $k_{tt}, k_{0t}, k_{t0}, k_{00}$ form the components of an actual stiffness matrix and are arranged as

$$k = \begin{bmatrix} k_{tt} & k_{t0} \\ k_{0t} & k_{00} \end{bmatrix} \tag{6.4}$$

and

$$k_{0t} = k_{t0}{}^{-1} \tag{6.5}$$

where k_{tt} represents the stiffness matrix corresponding to DOF's with non-zero masses and k_{00} represents the stiffness matrix of DOF's with zero masses.

Using static condensation, the number of active DOF's obtained for the full-model and reduced-model are 294 and 149 respectively.

To account for the damping of the bridge, Rayleigh damping is applied to the system. Typically, 1.5% - 2% damping is considered as the inherited damping for a bridge structure. Assuming 1.5% damping ratio for the Quincy Bayview Bridge, the damping matrix is developed as follows (Chopra, 2013)

$$c = a_0 m + a_1 k \tag{6.6}$$

where a_0 and a_1 represent the coefficients that are dependent on the particular modal frequencies of the system.

$$a_0 = \zeta \frac{2\omega_i \omega_j}{\omega_i + \omega_j} \tag{6.7}$$

and

$$a_1 = \zeta \frac{2}{\omega_i + \omega_j} \tag{6.8}$$

To consider the damping of the subsystems such as for HDRB isolators and linear viscous dampers, the damping coefficient of the subsystems is added to the corresponding DOF's of the system.

6.2 State-Space Formulation

The equation of motion can get cumbersome to solve for higher order systems i.e. systems that include large degrees of freedom such as a cable-stayed bridge. Therefore, state-space formulation is carried out to breakdown the N degree of freedom system into a set of first order equations that involve state variables. Therefore, representing a system in the form of state-space gives the advantage of solving any multivariable nonlinear system as a first order system,

irrespective of its order, with efficient design and analysis. The state equations are set up in a matrix form as mentioned below (Connor, 2003)

$$X = \begin{bmatrix} u \\ \dot{u} \end{bmatrix} = X(t) \tag{6.9}$$

where u and $\dot{u}$ are the displacements and velocities of the structure. Therefore, the equilibrium equation in the matrix notation can be written as

$$\frac{dX}{dt} = \dot{X} = AX + B_f F + B_g a_g + B_p p \tag{6.10}$$

The coefficient matrices are defined as

$$A = \begin{bmatrix} O & I \\ -M^{-1}K & -M^{-1}C \end{bmatrix} \tag{6.11}$$

$$B_f = \begin{bmatrix} O \\ M^{-1}E_f \end{bmatrix} \tag{6.12}$$

$$B_g = \begin{bmatrix} O \\ -E \end{bmatrix} \tag{6.13}$$

$$B_p = \begin{bmatrix} O \\ M^{-1} \end{bmatrix} \tag{6.14}$$

where M, K, C represent the mass, stiffness and damping matrix of the structure. E_f is the placement matrix consisting of zeros and ones. The ones in the matrix indicate the locations where the forces are to be acted on the respective degrees of freedom. p represents the external force acting on the system, a_g is the acceleration of the seismic excitation and E is a vector of ones whose order depends on the order of the system. O is the zero matrix and I is the identity matrix with size as that of M .

The C matrix is dependent on the control system implemented on the bridge. For passive control, the contribution from HDRB and linear viscous damper is also taken into consideration for the specific degree of freedom.

6.3 MATLAB® and SIMULINK®

The computational tools such as MATLAB and SIMULINK have been utilized to process the modal parameters such as mass and stiffness data obtained from SAP2000. Earthquake acceleration data, Static condensation, Rayleigh damping and input for state space formulation is set up to run in MATLAB. The input from MATLAB is then transferred to SIMULINK that consists of a simulated structure of the model, uncontrolled and controlled plant, SAC and MR Damper is created using mathematical formulations involved in their design. The model developed for MR Damper and SAC are shown in Figure 5.1 and Figure 5.2.

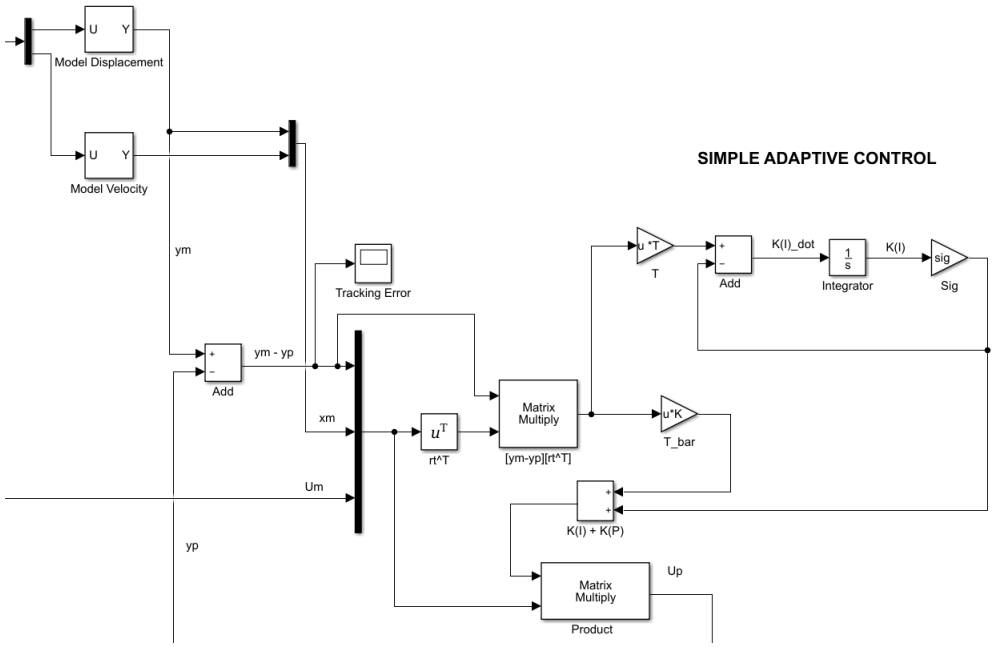

Figure 6.1: Schematic representation of SAC in SIMULINK®

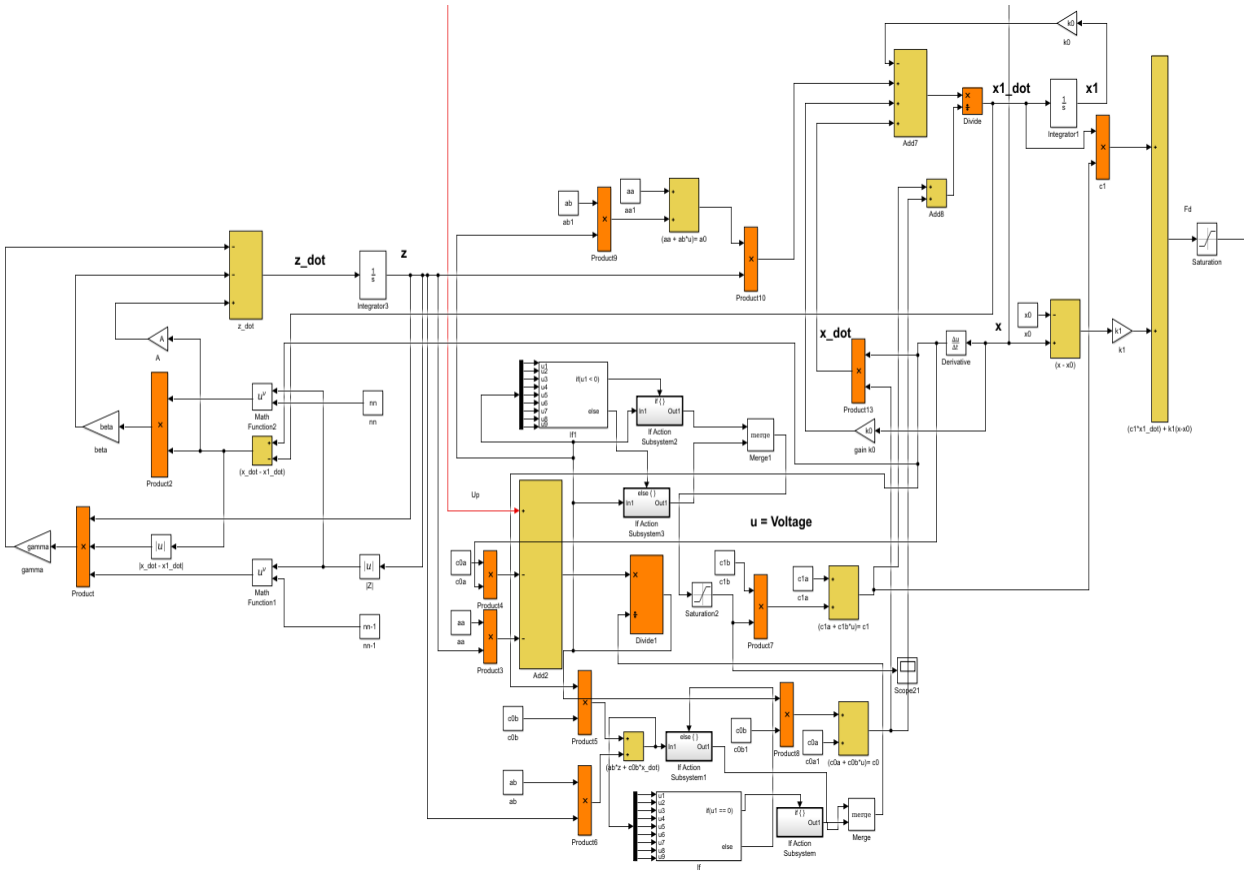

Figure 6.2: Schematic representation of a MR Damper in SIMULINK®

7. RESULTS AND CONCLUSIONS

The evaluation of the control strategies is carried out by comparing the responses of the isolator displacements at the deck-tower connection (y_1) and at the abutment (y_2) and the isolator velocities at the deck-tower connection ($\dot{y}_1$) and at the abutment ($\dot{y}_2$) for the 1940 El Centro and the 1994 Northridge Earthquakes in the transverse direction. The displacements and velocities experienced by the bridge in the longitudinal direction are very small when compared to the transverse, and therefore is considered negligible and is not discussed in detail.

7.1 Evaluation of the hybrid control strategies

Table 7.1 and Table 7.3 give a measure of maximum responses of the uncontrolled, passive hybrid controlled and semi-active hybrid controlled bridge for the complete and reduced models. The abutments of the bridge are observed to experience greater displacements in comparison with the deck-tower connection. This can be accredited to the rigidity offered by the towers due to the presence of the upper and lower struts. It can also be noted that the responses of the structure are highly dependent on the intensity of the earthquake. The near field earthquake with a high PGA value led to higher displacements than the far-field earthquake.

The hybrid control strategy is found to significantly reduce the displacements of the bridge compared to the uncontrolled model. A similar reduction in displacements is observed between the passive hybrid and the semi-active hybrid control strategy. The performance of the MR Dampers is observed to be on par with the idealized linear viscous dampers. The force exerted by the LVD varies linearly with its velocity and has a constant damping matrix. The devices do not

have any restrictions on the forces generated. Therefore, it can be concluded that the MR Dampers have the efficiency to deliver performance of an idealized passive device, which in reality is not a practical device.

The maximum velocities experienced by the isolators placed at the deck-tower and abutment connections for the full and reduced models are tabulated in Table 7.2 and Table 7.4 respectively. Similar to the displacement responses, the abutments experience greater seismic effects than the deck-tower connections. The bridge is expected to be severely damaged when hit by an earthquake with an acceleration record similar to the 1994 Northridge Earthquake. Therefore, it is very important to design a structure to deliver a favorable response for a varied seismic excitation. The passive and semi-active hybrid control have shown to effectively improve the performance of the bridge.

Table 7.1: Maximum displacements of the uncontrolled, passive hybrid and semi-active hybrid control for the full-model of Quincy Bayview Bridge.

Earthquake	Response Quantity	Uncontrolled	Passive Hybrid HDRB + LVD	Semi-Active Hybrid HDRB + MR Damper (SAC)
El Centro	y_1 (ft)	0.213	0.163	0.173
	y_2 (ft)	4.415	1.186	1.598
Northridge	y_1 (ft)	0.359	0.343	0.342
	y_2 (ft)	7.492	1.743	2.577

Table 7.2: Maximum velocities of the uncontrolled, passive hybrid and semi-active hybrid control for the full-model of Quincy Bayview Bridge.

Earthquake	Response Quantity	Uncontrolled	Passive Hybrid HDRB + LVD	Semi-Active Hybrid HDRB + MR Damper (SAC)
El Centro	$\dot{y}_1$ (ft/sec)	7.353	6.999	7.147
	$\dot{y}_2$ (ft/sec)	86.54	26.41	29.06
Northridge	$\dot{y}_1$ (ft/sec)	9.388	8.322	8.594
	$\dot{y}_2$ (ft/sec)	156.1	46.09	51.85

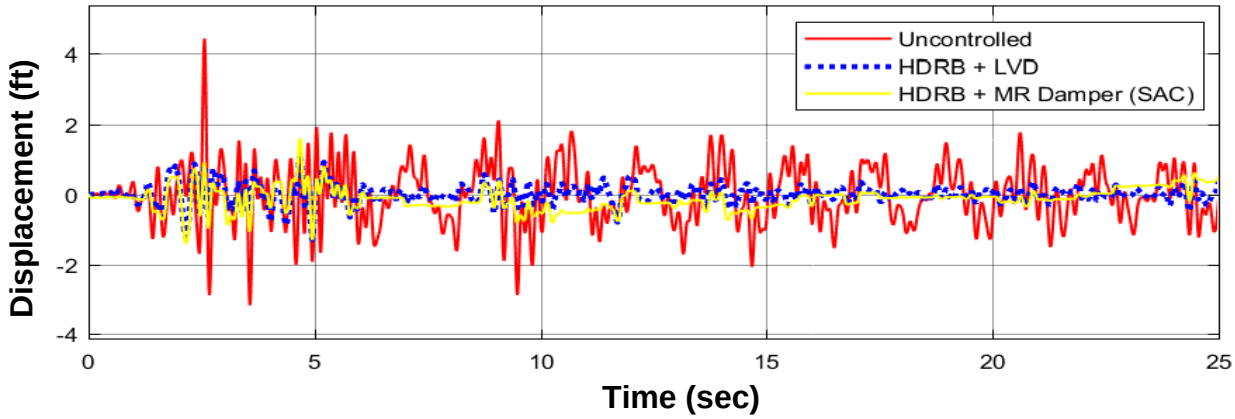

Figure 7.1: Displacement response of the isolator at abutment in the transverse direction for the full model, El Centro Earthquake.

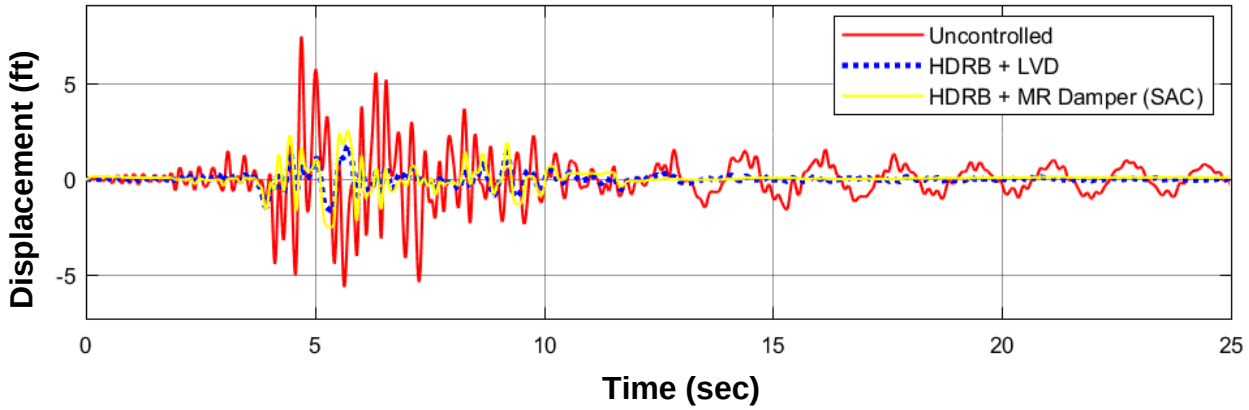

Figure 7.2: Displacement response of the isolator at abutment in the transverse direction for the full model, Northridge Earthquake.

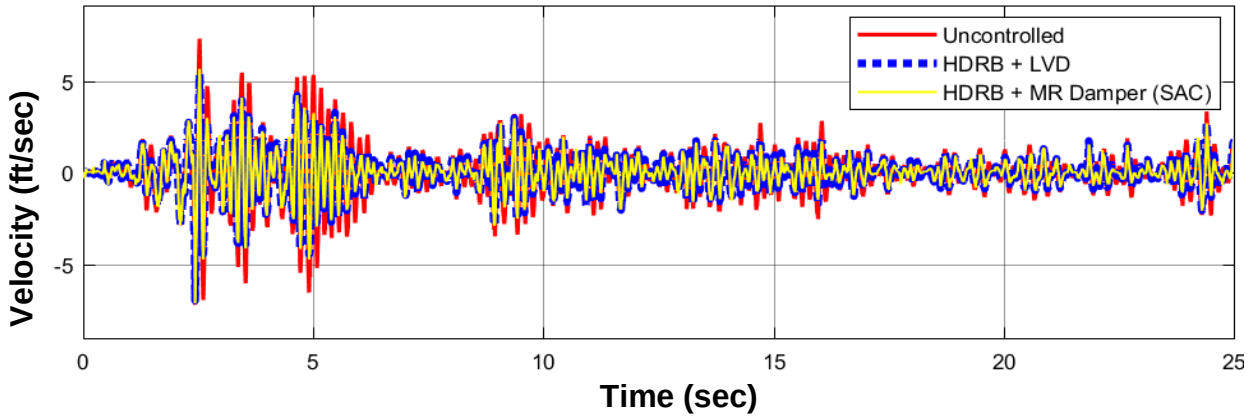

Figure 7.3: Velocity response of the isolator at deck-tower connection in the transverse direction for the full model, El Centro Earthquake.

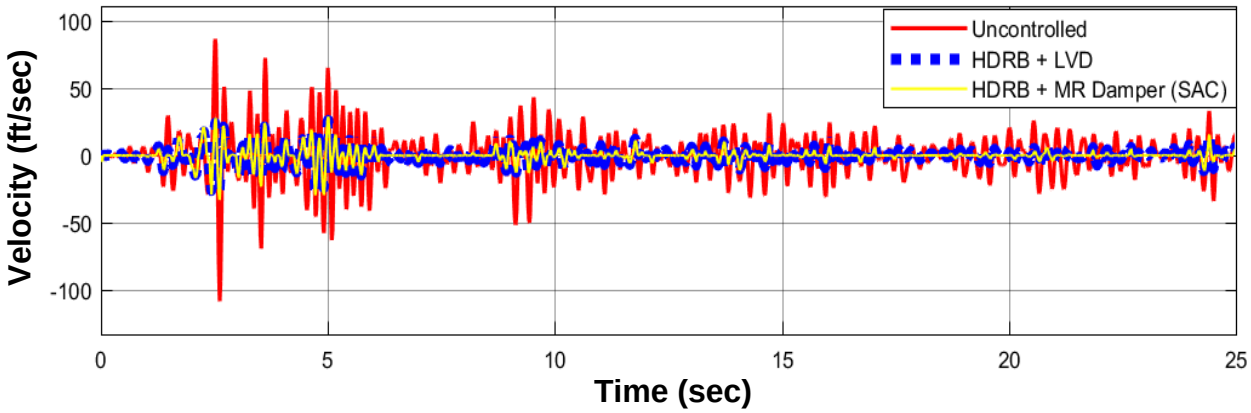

Figure 7.4: Velocity response of the isolator at abutment in the transverse direction for the full model, El Centro Earthquake.

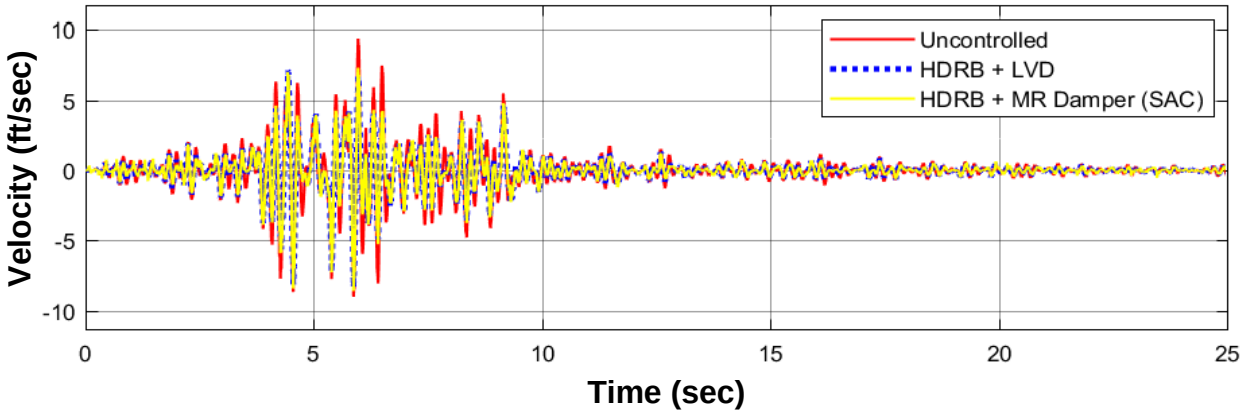

Figure 7.5: Velocity response of the isolator at deck-tower connection in the transverse direction for the full model, Northridge Earthquake.

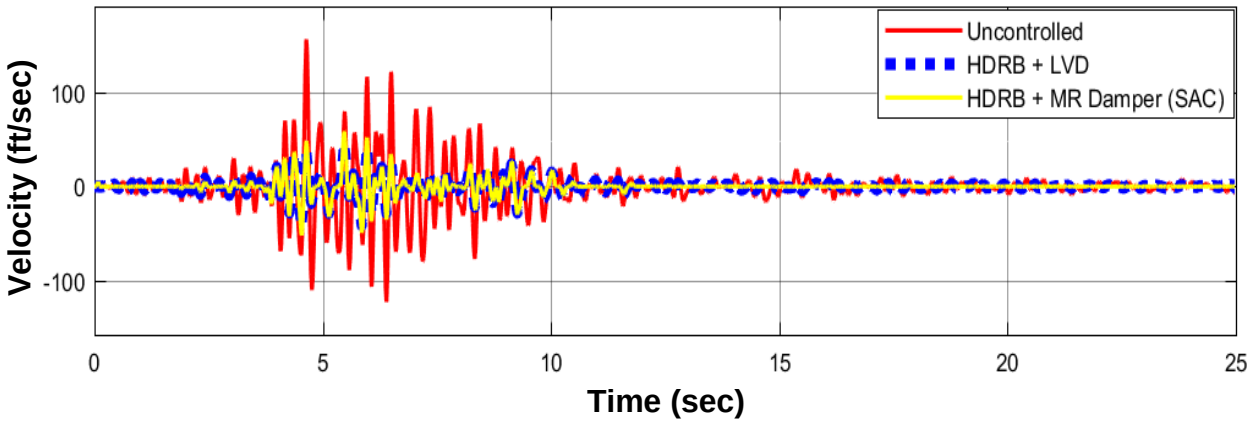

Figure 7.6: Velocity response of the isolator at abutment connection in the transverse direction for the full model, Northridge Earthquake.

Table 7.3: Maximum displacements of the uncontrolled, passive hybrid and semi-active hybrid control for the reduced-model of Quincy Bayview Bridge

Earthquake	Response Quantity	Uncontrolled	Passive Hybrid HDRB + LVD	Semi-Active Hybrid HDRB + MR Damper (SAC)
El Centro	y_1 (ft)	0.031	0.026	0.022
	y_2 (ft)	0.367	0.209	0.167
Northridge	y_1 (ft)	0.076	0.052	0.05
	y_2 (ft)	0.564	0.453	0.43

Table 7.4: Maximum velocities of the uncontrolled, passive hybrid and semi-active hybrid control for the reduced-model of Quincy Bayview Bridge

Earthquake	Response Quantity	Uncontrolled	Passive Hybrid HDRB + LVD	Semi-Active Hybrid HDRB + MR Damper (SAC)
El Centro	$\dot{y}_1$ (ft/sec)	1.483	1.462	1.411
	$\dot{y}_2$ (ft/sec)	17.832	10.673	9.581
Northridge	$\dot{y}_1$ (ft/sec)	2.26	1.678	1.667
	$\dot{y}_2$ (ft/sec)	13.88	10.75	12.37

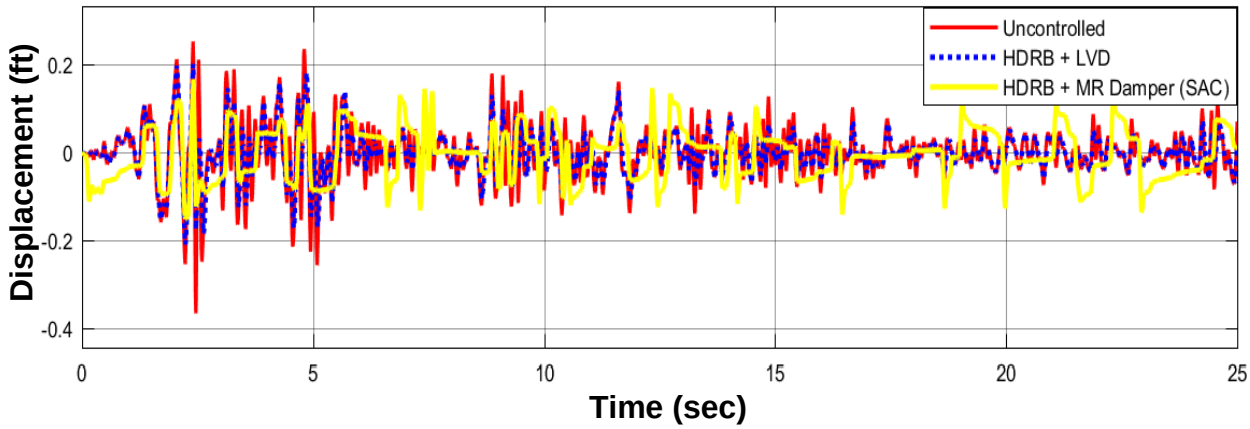

Figure 7.7: Displacement response of the isolator at abutment in the transverse direction for the reduced model, El Centro Earthquake.

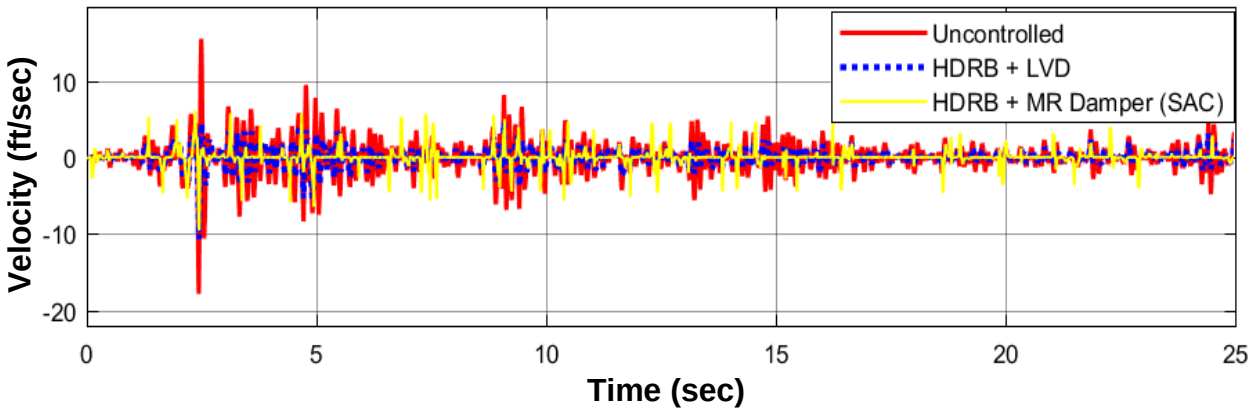

Figure 7.8: Velocity response of the isolator at abutment in the transverse direction for the reduced model, El Centro Earthquake.

7.2 Evaluation of passive, semi-active and hybrid control

To study the efficiency exhibited by the hybrid control, the passive hybrid and semi-active hybrid strategies are compared with the individual performances of the HDRB and the MR Dampers for the reduced and full model of the bridge. As observed from Table 7.5 and Table 7.6, the hybrid strategies perform better in alleviating the response than the passive and semi-active control. For the full model of the bridge, the hybrid control reduces the displacements by 20% at the deck-tower connections and by 70% at the abutments due to the disturbances caused by the El Centro earthquakes. The response reduction attained by the semi-active and passive is found to be widely varied with the passive performing better than the semi-active.

For the reduced model of the bridge, 15% - 30% reduction in displacements was observed at the deck-tower connections and about 40% - 50% reduction at the abutments. A similar percentage reduction was observed for the velocity responses of the bridge as the result of the seismic excitation. For the reduced model, the semi-active strategy delivered a better response than the passive strategy.

No decisive conclusion can be drawn about the individual structural performances of the passive and semi-active device for the given seismic excitations. Furthermore analysis, such as studying the response of the system for various intensity earthquakes and considering parametric variations in the system, will be required to distinctly comment on the behavior of these devices.

Table 7.5: Peak displacement and velocity responses for the full-model.

Earthquake	Response Quantity	Passive HDRB	Semi-active MR Damper	Passive Hybrid HDRB + LVD	Semi-Active Hybrid HDRB + MRD (SAC)
El Centro	y_1 (ft)	0.186	0.192	0.163	0.173
	y_2 (ft)	1.614	3.720	1.186	1.598
Northridge	y_1 (ft)	0.337	0.329	0.343	0.342
	y_2 (ft)	2.668	6.973	1.743	2.577
El Centro	$\dot{y}_1$ (ft/sec)	7.300	7.170	6.999	7.147
	$\dot{y}_2$ (ft/sec)	41.840	73.110	26.410	29.060
Northridge	$\dot{y}_1$ (ft/sec)	8.972	8.674	8.322	8.594
	$\dot{y}_2$ (ft/sec)	54.340	56.060	46.090	51.850

Table 7.6: Peak displacement and velocity responses for the reduced-model.

Earthquake	Response Quantity	Passive HDRB	Semi-active MR Damper	Passive Hybrid HDRB + LVD	Semi-Active Hybrid HDRB + MRD (SAC)
El Centro	y_1 (ft)	0.027	0.026	0.026	0.022
	y_2 (ft)	0.247	0.188	0.209	0.167
Northridge	y_1 (ft)	0.058	0.066	0.052	0.050
	y_2 (ft)	0.508	0.491	0.453	0.430
El Centro	$\dot{y}_1$ (ft/sec)	1.445	1.457	1.462	1.411
	$\dot{y}_2$ (ft/sec)	13.330	11.620	10.673	9.581
Northridge	$\dot{y}_1$ (ft/sec)	1.728	1.735	1.678	1.667
	$\dot{y}_2$ (ft/sec)	11.850	12.070	10.750	12.370

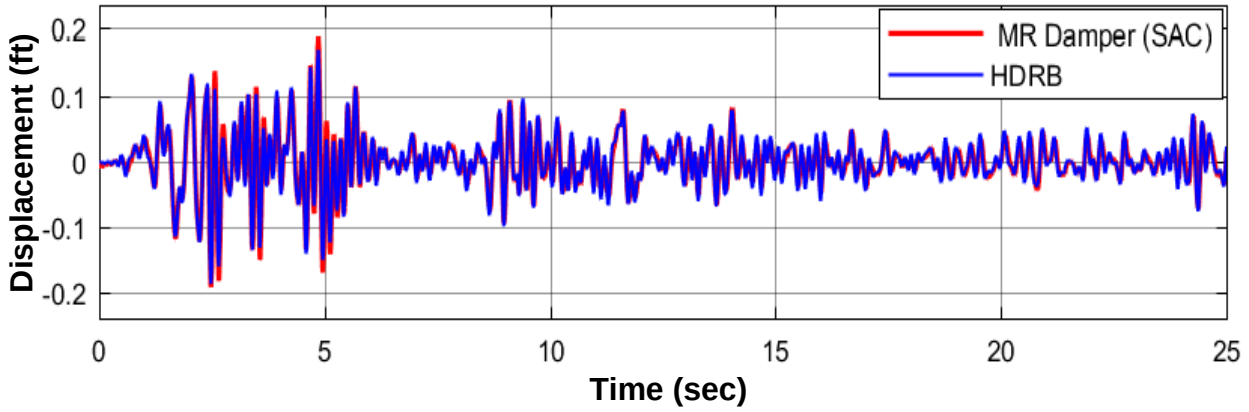

Figure 7.9: Displacement response at the deck-tower connection in the transverse direction for the full model, El Centro Earthquake.

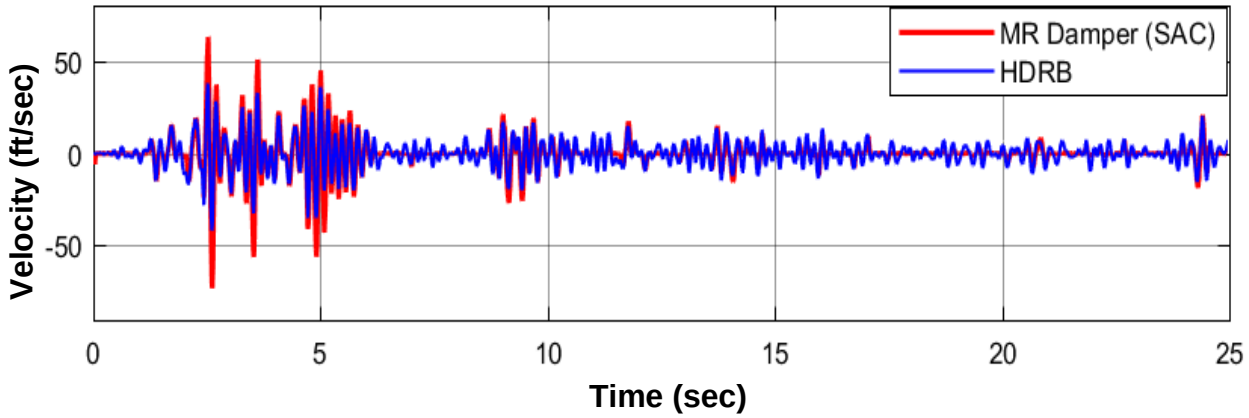

Figure 7.10: Velocity response at the abutment in the transverse direction for the full model, El Centro Earthquake.

7.3 Evaluation of semi-active hybrid with passive-on and passive-off

As discussed above, the critical responses for the bridge were attained at the abutments. Therefore, the response in these locations have also been investigated for two passive cases - passive-on and passive-off for the MR Damper. The MR Damper with passive-on is found to deliver a response similar to the MR Damper controlled by SAC. Due to the minimum voltage supply, the forces generated by the passive-off damper are lesser than the other cases. Hence, the

displacements and velocities observed for passive-off are higher than the passive-on and the MR Damper controlled with SAC.

Table 7.7: Peak responses at the abutment for full model of the bridge

Earthquake	Response Quantity	HDRB + MR Damper (SAC)	HDRB + MR Damper (Passive On)	HDRB + MR Damper (Passive Off)
El Centro	y_2 (ft.)	1.598	1.612	1.453
	$\dot{y}_2$ (ft./sec)	29.060	28.480	33.700
Northridge	y_2 (ft.)	2.577	2.568	2.782
	$\dot{y}_2$ (ft./sec)	51.850	52.621	54.23

Table 7.8: Peak responses at the abutment for reduced model of the bridge

Earthquake	Response Quantity	HDRB + MR Damper (SAC)	HDRB + MR Damper (Passive On)	HDRB + MR Damper (Passive Off)
El Centro	y_2 (ft.)	0.167	0.147	0.211
	$\dot{y}_2$ (ft./sec)	9.580	9.652	10.458
Northridge	y_2 (ft.)	0.431	0.431	0.476
	$\dot{y}_2$ (ft./sec)	12.370	12.460	11.350

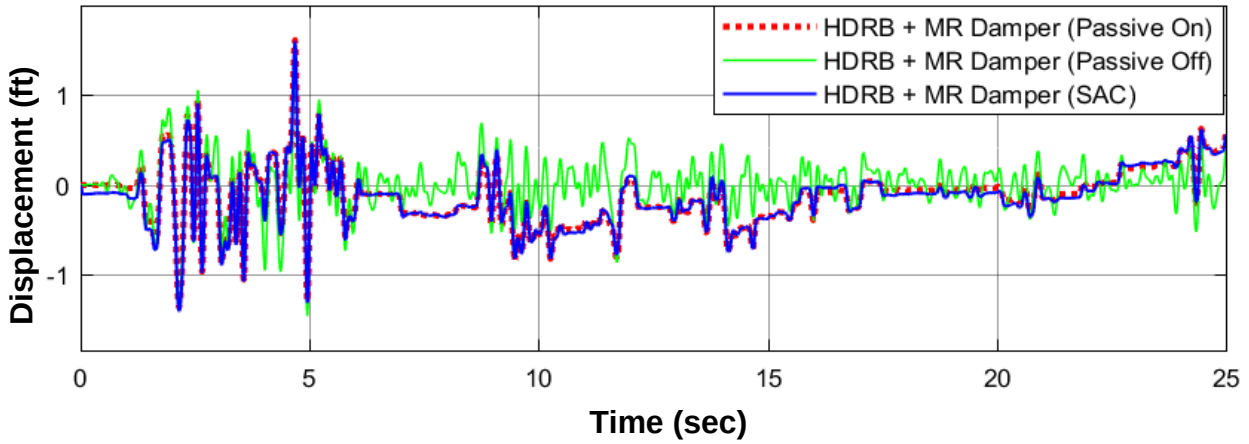

Figure 7.11: Displacement response at the abutment in the transverse direction for full model, El Centro Earthquake.

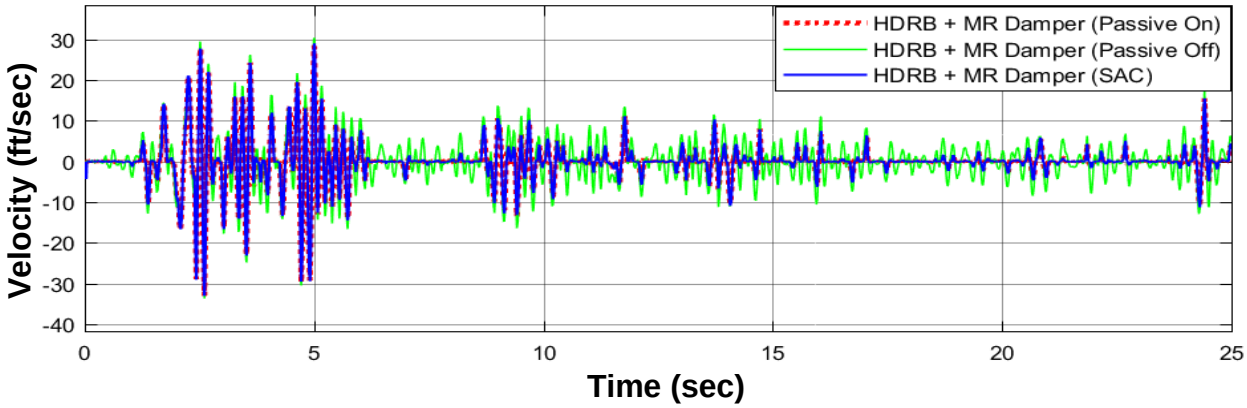

Figure 7.12: Velocity response at the abutment in the transverse direction for the full model, El Centro Earthquake.

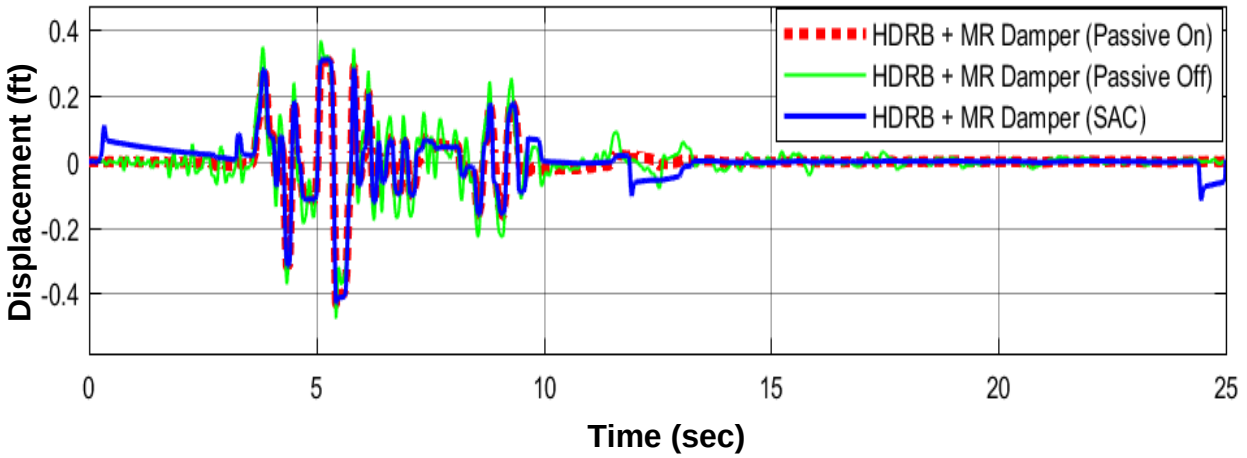

Figure 7.13: Displacement response of the abutment in the transverse direction for the reduced model, Northridge Earthquake.

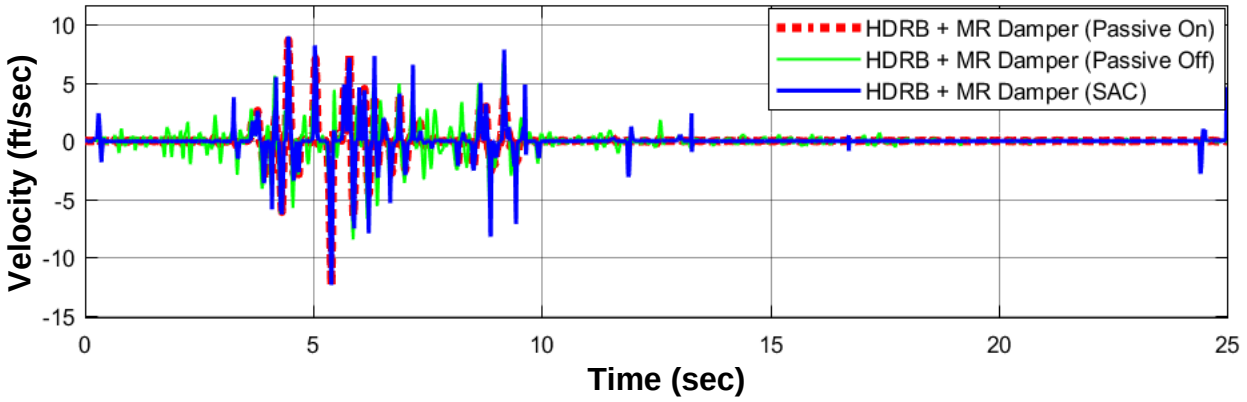

Figure 7.14: Velocity response of the abutment in the transverse direction for the reduced model, Northridge Earthquake.

The forces generated by the MR Damper contributes significantly towards the response of the structure to the control strategies applied. It is highly dependent on the input voltage supplied. For the passive-on case, the MR Damper operated for a voltage of 10 V whereas for the passive-off case, a voltage of 0 V is applied. In the case of semi-active hybrid, the MR Damper was applied a voltage ranging from 0 V to 10 V.

Table 7.9 shows the maximum forces generated by the control devices. It is observed that for an idealized linear viscous damper, a maximum force of 4×10^5 kips is produced whereas the MR Damper generates a maximum force of 2.248×10^5 kips. for the semi-active and passive-on case. For the passive-off, the MR Damper generates a force of 3.34×10^4 kips. Therefore, it can be justified that the due to the higher forces generated by the idealized linear viscous damper, a better performance is achieved by the passive hybrid control than the semi-active hybrid control. The forces generated by the MR Damper for a voltage of 0 V is less and therefore, the response reduction is lesser than that for the other control strategies.

Table 7.9: Maximum control forces generated by devices for full model, El Centro Earthquake

Maximum Control Forces Generated (kips)			
HDRB + LVD	HDRB + MR Damper (SAC)	HDRB + MR Damper (Passive-on)	HDRB + MR Damper (Passive-off)
4×10^5	2.248×10^5	2.248×10^5	3.34×10^4

7.4 Evaluation of full-model and reduced-model

In an attempt to reduce the computational effort and due to the symmetric modal behavior of the bridge, a partial model of the bridge is created for the implementation of control strategies. The end conditions of the bridge are defined in a way that it captures the modal behavior of the full bridge. With this hypothesis, the percentage reduction in the displacement and velocity

responses for both the models are calculated and tabulated in Table 7.9. The table compares the response reduction for the hybrid control strategies.

The variation in the percentage reduction proves that the partial model is not the best approach to substitute the full-scale cable-stayed bridge and such a difference in response can be attributed to the failure in extensively capturing the complete geometric and material non-linearity of the structural components of the bridge and the complex dynamic behavior exhibited by the cable-stayed bridge. A much accurate alternate solution that can be suggested to represent the behavior of the full structure and to simultaneously reduce the computational effort would be to scale down the structure and the seismic excitation accordingly for the analysis.

Table 7.10: Peak response percentage reduction of full and reduced model for hybrid strategies

		Full Model		**Reduced Model**	
Earthquake	**Response Quantity**	**Passive Hybrid HDRB + LVD**	**Semi-active Hybrid HDRB + MR Damper**	**Passive Hybrid HDRB + LVD**	**Semi-active Hybrid HDRB + MR Damper**
El Centro	y_1	23%	19%	16%	29%
	y_2	73%	64%	43%	54%
Northridge	y_1	4%	5%	32%	34%
	y_2	77%	66%	20%	24%
El Centro	$\dot{y}_1$	5%	3%	1%	5%
	$\dot{y}_2$	70%	67%	40%	46%
Northridge	$\dot{y}_1$	11%	8%	26%	26%
	$\dot{y}_2$	70%	67%	23%	11%

7.5 Summary and future work

In this thesis, the simple adaptive control algorithm has been executed as a semi-active hybrid control strategy to evaluate the reduction in seismic response of the Quincy Bayview Bridge in Illinois. As part of control mechanism, the bridge is simulated with idealized passive control devices such as HDRB and LVD placed at the support locations of the bridge, i.e. at the deck-tower connections and at the abutments. Semi-active devices such as Magnetorheological dampers are located at the supports in the longitudinal and transverse direction.

The performance of the semi-active controlled bridge (HDRB + MR Damper) was compared with its uncontrolled model. It was observed that the semi-active hybrid control strategy reduced the response of the bridge efficiently. When compared with the passive hybrid strategy (controlled using HDRB + LVD), the reduction obtained was on a similar scale. It is contemplated that the idealized scenario of the passive devices allows it to generate large forces which results in reducing the response of the structure on par with the controlled MR Dampers. The efficiency of MR Dampers, controlled with SAC, is demonstrated as it exhibits a performance close to a passive idealized device.

The performance of the MR Damper, controlled with SAC, has also been studied for additional passive cases such as for passive-on and passive-off. The MR Damper generates maximum forces when it is controlled with SAC and for passive-on in comparison with passive-off and hence displays better reduction in response than the passive-off.

Additionally, the thesis also focuses on reducing the computational efforts for the structure by designing a reduced model such that it captures the modal behavior of the complete structure. The reduced model is then analyzed similarly for the passive hybrid and semi-active hybrid control strategies and the percentage reduction for the complete and reduced model are compared. The

difference in percentage reduction validates that the reduced model cannot be substituted for the complete model. It is probable that the former fails to capture the geometric and material non-linearity of the latter. The complex dynamic behavior of a cable-stayed bridge is challenging to capture extensively.

The future work of this thesis would involve developing the scope of modeling a reduced structure of a cable-stayed bridge to meet its computational challenges. Furthermore, the complete and reduced structure can be evaluated for the seismic response reduction when controlled using passive (HDRB) and semi-active devices (MR Dampers) for various earthquake excitations and parametric changes to arrive at a conclusion depicting the efficient control strategy of the two.

REFERENCES

Adeli, H, and J. Zhang. 1995. "Fully nonlinear analysis of composite girder cable-stayed bridges." *Computers & Structures* 267-277.

Agrawal, A., Ping. Tan, S. Nagarajaiah, and Jian Zhang. 2009. "Benchmark structural control probem for a seismically excited highway bridge-Part 1:Phase 1 problem defintion." *Structural Control and health monitoring* 509-529.

Agrawal, A.K., and W.L He. June 25-27, 2001. "Control of seismically excited cable-stayed bridge using a resetting semi-active stiffness damper." *American Control Conference.* Arlington, VA.

Ali, H.M., and A.M. Abdel-Ghaffar. 1995. "Seismic passive control of cable-stayed bridges." *Shock and vibration* 259-272.

Anderson, E.L., and S.A. Mahin. August 1-6, 2004. "An evaluation of bi-directional earthquake shaking on the provisions of the AASHTO guide speficiations for seismic isolation design." *13th World conference on earthquake engineering.* Vancouver, B.C., Canada.

Asai, T. 2014. *Structural control strategies for earthquake response reduction of buildings.* PhD Thesis, Urbana, Illinois: ProQuest LLC.

Asgari, B., S.A. Osman, and A. Adnan. 2013. "Three-dimensional finite element modelling of long-span cable-stayed bridges." *The IES journal Part A: Civil & Structural Engineering* 258-269.

B.B, Soneji, and Jangid R.S. 2006. "Passive hybrid systems for earthquake protection of cable-stayed bridge." *Engineering Structures.*

Barkana, I. 2015. "Adaptive Control? But is so Simple! A tribute tothe efficiency, simplicity andbeauty of adaptive control." *Journal of intelligent and robotic systems.*

Bitaraf M, Barroso L.R., Hurlebaus S. 2010. "Adaptive control to mitigate damage imoact on strutural response." *Journal of intelligent material systems and structures.*

Bitaraf, M, and S Hurlebaus. 2013. "Semi-active adaptive control of seismically excited 20-story nonlinear building." *engineering structures* 2107-2118.

Bitaraf, M, S Hurlebaus, and L.R. Barroso. 2012. "Acrive and semi-active adaptive control for undamaged and damaged building structures under seismic load." *Computer-aided civil and infrastructure engineering* 48-64.

Bitaraf, M. 2011. *Enhancing the structural performance with active and semi-active devices using adaptive control strategy.* PhD Thesis, Ann Arbor: ProQuest.

Cardenas, R.A., J.C. Viramontes, A.D. Gonzalez, and G.H. Ruiz. 2008. "Analysis for the optimal location of cable damping systems on stayed bridges." *Nonlinear Dynamics* 347-359.

Chang, C, and C Loh. 2006. "Seismic response control of cable-stayed bridge using different control strategies." *Journal of earthquake engineering* 481-508.

Chopra, A.K. 2013. *Dynamics of Structures- Theory and applications to earthquake engineering fourth edition.* Essex: Pearson education limited.

Connor, J.J. 2003. *Introduction to structural motion control.* New Jersey: Pearson Education, Inc.

Dicleli, M., and M.C. Constantinou. 2005. "Efficiency of seismic isolation for seismic retrofitting of heavy substructured bridges." *Journal of bridge engineering* 429-441.

Dutta, A.K., A. Dutta, and S.K. Deb. 2008. "Design of an active controller for Quincy Bayview Bridge, Illinois, USA against seismic excitation-Part 1: Model Updating." *Structural control and health monitoring* 1057-1077.

Dyke, S.J., B.F. Spencer Jr., M.K. Sain, and J.D. Carlson. 1996. "Modeling and control of magnetorheological dampers for seismic response reduction." *Smart materials structures* 565-575.

Franklin, G.F., J.D. Powell, and A.E. Naeini. 2002. *Feedback control of dynamic systems.* New Jersey: Prentice Hall.

Freeman, S.A. 2007. "Response spectra as a useful design and analysis tool for practicing structural engineers." *ISET Journal of earthquake technology* 25-37.

He, W.L., and A.K. Agrawal. 2007. "Passive hybrid control systems for seismic protection of a benchmark cable-stayed bridge." *Structural control and health monitoring* 1-26.

Horwich, G. 2000. "Economic Lessons of the Kobe Earthquake." *Economic development and cultural change* (The university of chicago press) 521-542.

Hu, J., I. Harik, S.W. Smith, J. Gagel, Campbell J.E., and R.C. Graves. 2006. *Baseline modeling of the owensboro cable-stayed bridge over the ohio river.* Research Report, Lexington: Kentucky Transportation Center.

J, Wilson, and Liu T. 1991. "Ambient vibration measurements on a cable-stayed bridge." *Earthquake Engineering and Structural Dynamics* 723-747.

J.N., Yang, Kim J.H., and Agrawal A.K. December 2000. "Resetting semiactive stiffnes damper for seismic response control." *Journal of structural engineering* 1427-1433.

Jung, H.J., K.S. Park, B.F. Spencer Jr, and I.W. Lee. 2004. "Hybrid seismic protection of cable-stayed bridges." *Earthquake engineering and structural dynamics* 795-820.

K, Villarreal, Wilson C, and Abdullah M. 2005. *Effects of MR Damper placment on structure vibration parameters.* January. https://www.researchgate.net/publication/241219802.

M, Bitaraf, Ozbulut O, Hurlebaus S, and Barroso L. 2010. "Application of semi-active control strategies for seismic protection of buildings with MR Dampers." *Engineering Structures* 3040-3047.

Mahdi, A., and P.O Abdelhafid. 2015. "Seismic response reduction using semi-active magneto-rheological dampers." *French Vietnamese conference Innovations in construction.* Paris.

Park, K, H., Spencer Jr, B.F. Jung, and I Lee. 2003. "Hybrid control of seismic protection of a phase II benchmark cable-stayed bridge." *Journal of structural control* 231-247.

Park, K.S., H.J. Jung, and I.W. Lee. 2003. "Hybrid control strategy for seismic protection of a benchmark cable-stayed bridge." *Engineering Structures* 405-417.

Park, K.S., I.W. Lee, H.J. Jung, and J.G. Park. 2003. "Integrated passive-active system for seismic protection of a cable-stayed bridge." *Journal of earthquake engineering* 615-633.

Poynor, J. n.d. *Innovative desigs for magneto-rheological dampers.* Thesis, Virginia: Virginia Polytechnic Institute and State University.

Pridham, B.A., and J.C. Wilson. 2005. "A reassessment of dynamic characteristics of the quincy bayview bridge using output-only identification techniques." *Earthquake engineering and structural dynamics* 787-805.

Ruangrassamee, A., and K Kawashima. 2008. "Seismic response control of a cable-stayed bridge by variable dampers." *Journal of earthquake engineering* 153-165.

Saaed, T.E., G. Nikolakopoulos, J. Jonasson, and H. Hedlund. 2015. "A state-of-the-art review of structural control systems." *Journal of vibration and control* 919-937.

Salem, M.M.A. May 2014. *Seismic response control of structures using semi-active and passive variable stiffness devices.* PhD Thesis, Ann Arbor: ProQuest LLC.

Shiba, K., S. Mase, Y Yabe, and K Tamura. 1998. "Active/passive vibration control systems for tall buildings." *Smart materials and structures* 588-598.

Soneji, B.B, and R.S. Jangid. 2007. "Passive hybrid systems for earthquake protection of cable-stayed bridge." *Engineering structures* 57-70.

Soneji, B.B, and R.S. Jangid. 2006. "Seismic control of cable-stayed bridge using semi-active hybrid system." *Bridge Structures* 45-60.

Spencer Jr., B.F., S.J. Dyke, M.K. Sain, and J.D. Carlson. March 1997. "Phenomenological model for magnetorheological dampers." *Journal of engineering mechanics* .

Tewari, Ashish. 2002. *Modern control design with MATLAB and SIMULINK*. England: John Wiley & Sons, Ltd.

Tierney, K.J. 1997. "Business Impacts of the Northridge Earthquake." *Journal of contingencies and management* 87-97.

Tubaldi, E., S.A. Mitoulis, and H. Ahmadi. 2018. "Comparison of different models for high damping rubber bearings in seismically isolated bridges." *Soil dynamics and earthquake engineering* 329-345.

Valdebenito, G.E., A.C. Aparicio, and J.J Alvarez. 2012. "Sesimic response of cable-stayed bridges for different layout conditions: A comparative analysis." *The 15th World conference on earthquake engineering.* Lisboa.

Valdebenito, G.E., Aparicio, A.C. October 12-17, 2008. "Effect of variation of the stay prestressing forces on the seismic response of cable-stayed bridges." *The 14th world conference on earthquake engineering.* Beijing, China.

Wesolowsky, M.J., and J.C. Wilson. 2003. "Seismic isolation of cable-stayed bridges for near-field ground motions." *Earthquake engineering and structural dynamics* 2107-2126.

Wilson, J.C., and W. Gravelle. 1991. "Modelling of a cable-stayed bridge for dynamic analysis." *Earthquake Engineering and structural dynamics* 707-721.

Yi, F., and S.J. Dyke. June 2000. "Structural control systems: Performance Assessment." *American control conference.* Chicago, Illinois.

Zabala, J.L.M. 1996. *State space formulation for structural dynamics.* Thesis, MIT.

Ze-bing, D, H. Jin-zhi, and W. Hong-xia. 2004. "Semi-active control of a cable-stayed bridge under multiple-support excitations." *Journal of zhejiang University science* 317-325.

Zhang, J., J. Prader, K.A. Grimmelsman, F.Moon, A.E.Aktan, and A. Shama. 2009. "Challenges in experimental vibration analysis for structural identification and corresponding engineering strategies."